Supporting Information

*Brandon Watson, Olivia Grounds, William Borley, Sergiy V. Rosokha**[1]

Resolving Halogen vs Hydrogen Bonding Dichotomy in Solutions: Intermolecular Complexes of Trihalomethanes with Halide and Pseudohalide Anions

Department of Chemistry, Ball State University, Muncie, IN, USA, 47306

Table of Content

[1] Corresponding author, e-mail: svrosokha@bsu.edu, phone: + 1-765-285-8615.

Calculation of the equilibria constants

Formation constants of the XB and/or HB complexes [CHX_3, A^-] (X = Cl, Br, I, A = Cl, Br. I, NCS, NCO, N_3) were established via UV-Vis and NMR measurements of the acetonitrile solutions containing constant concentrations (from 2 to 5 mM) of CHX_3 and variable concentrations (from 0 to ~ 0.4M) of tetrapropyl-ammonium salts of (pseudo-)halide anions, A^-.[2] Several series of measurements were also done with n-Bu_4NA salts, and they afforded the same, within accuracy limit, formation constants as the corresponding measurements with Pr_4NA.[3] For the UV-Vis experiments, 10.0 mL of a stock solution of CHX_3 (10.0 mM) and 5.00 mL of solution of Pr_4NA (from 0.4 M to 0.8 M) were typically prepared. Then, 0.500 mL of the stock solution of CHX_3 were mixed in a microvolumetric (1.00 mL) flask with x mL of stock solution of Pr_4NA and (0.500-x) mL of acetonitrile (where x typically were 0.500, 0.400, 0.330, 0.250, 0.200, 0.160, 0.130, 0.100, 0.080, 0.065, 0.050, 0.035, 0.020 or similar numbers) using gas-tight microsyringes with capacities from 0.050 mL to 0.500 mL. UV-Vis measurements were carried out in acetonitrile at 22 ^oC using quartz (1-mm path length) spectroscopic cells on a CARY 500 spectrophotometer. A Dewar equipped with quartz lens was used for the measurements at +5 to -70 ^oC. The temperature was adjusted with an ethanol-liquid nitrogen bath (±0.5 K). Solutions of for the NMR measurements were prepared in a similar way. However, stock solutions of CHX_3 (10.0 mM, 5.00 mL) and (Pr_4NA 3 mL, from 0.4 M to 0.8 M) for NMR measurements were prepared in CD_3CN (containing internal TMS standard). Also, 0.250 mL of solution of CHX_3 were mixed with x mL Pr_4NA and (0.250-x) mL of CD_3CN, so the total volumes of solutions for NMR measurements were 0.5 mL. ^1H NMR measurements were performed on the 400 MHz NMR-ECZ400S spectrometer at 22 ^oC.

Alternatively, series of UV-Vis measurements were done by mixing 0.250 mL of the stock solution of CHX_3 (prepared as described above) with 0.250 mL of the stock solution of Pr_4NA in Teflon-capped (1 mm) cuvettes equipped with sidearm. Separately, 5.0 mL of the stock solution of CHX_3 was mixed with 5.0 mL of acetonitrile (so the concentration of the CHX_3 in this solution was the same as that in the cuvette). After first spectrum was measured, x ml portions of the diluted solution of CHX_3 (where x = 0.125, 0.150, 0.200, 0.250, 0.300, 0.400, 0.500, 0.600, 0.750, 0.900, 1.000, 1.500, 2.000 or similar number) were added progressively and the spectra were measured after each addition. Thus, regardless of the method of preparation of solutions for the UV-Vis and NMR measurements, the concentrations of CHX_3 were kept constant, and concentrations of Pr_4NA varied substantially in a series of measurements; and the values of formation constants derived from both types of the UV-Vis experiments were the same (within the accuracy limit).

---

[2] Specific concentration of CHX_3 and Pr_4NA salts for different donor/acceptor pairs are listed in figure captures (see Figure 1, Figure S1 – S6, S9)

[3] Control experiments with tetrapropylammonium tetrafluoroborate verified that variation of concentration of this non-bonding anion in its mixtures with trihalomethanes in acetonitrile has negligible effects (as compared to that of pseudo-halide anions) on the chemical shifts of the CHX_3 protons (see Figure 2).

The formation constants and spectral characteristics obtained (as in the earlier studies) assuming formation of only one type of complex represent average values from 3-5 series of UV-Vis or NMR experiments for each CHX_3/A^- pair. Each of such series typically included 8-10 points. UV-Vis absorption values measured at two wavelengths were normally used in the calculations. For the multivariable treatments of the UV and NMR data, the data from 2-3 series of measurements of each CHX_3/A^- pair (with the same concentration of trihalomethane) were combined and treated simultaneously.

Extinction coefficients ε for $[CHX_3,A]$ complexes, limiting proton NMR shifts and equilibrium constants of their formation, K_{UV}^{eff} and K_{NMR}^{eff}, (Table 1 and Table S1) were first calculated via the Benesi-Hildebrand procedure and, additionally, via regression analysis. These treatments were based, as in the previous studies, on the assumption that only one type (either XB or HB) of 1:1 complex is formed in solution, i.e. that the formation of other types of complexes can be neglected:

$$CHX_3 + A^- \overset{K_{eff}}{\rightleftharpoons} [CHX_3, A^-] \quad \text{(S1)}$$

The effective formation constant of the complex is expressed as

$$K_{eff} = C_{com} / ((C^o_D - C_{com})(C^o_A - C_{com})) \quad \text{(S2)}$$

where C_{com} is the concentration of the complex, and C^o_D and C^o_A are initial concentrations of CHX_3 and A^-, respectively. When $C^o_A >> C^o_D$, $C^o_A - C_{com} \approx C^o_A$. Therefore $K_{eff} = C_{com}/((C^o_D - C_{com})C^o_A)$. Thus,

$$K_{eff}(C^o_D - C_{com})C^o_A - C_{com} = 0 \quad \text{(S3)}$$

Or

$$C_{com} = K_{eff}C^o_D C^o_A / (K_{eff}C^o_D + 1) \quad \text{(S4)}$$

Taking into account that: $\Delta Abs = \varepsilon\, l\, C_{com}$, where ΔAbs is the absorbance of the complex at certain wavelength (obtained by subtraction of the absorption of components), and l is the length of the spectrophotometric cell, the latter can be rearranged as the Benesi-Hildebrand equation:

$$C^o_D/\Delta Abs = 1/(\varepsilon\, l) + \{1/(K_{UV}^{eff}\, \varepsilon l)\} \times 1/[C^o_A] \quad \text{(S5)}$$

The Benesi-Hildebrand treatments of the UV-Vis absorption data are illustrated below in Figures S1C-S6C. It should be noted that the Benesi-Hildebrand procedure provided reliable results only if one reactant is present in a great excess and the complexation of the other reactant (in deficit) is in the 20-80% range (which is difficult to obtain with K values of ~ 1 or less due to solubility limitations). Thus, to verify the values of K_{UV}^{eff} and ε, as well as to determine K_{NMR}^{eff} and $\Delta\delta_\infty$, we carried out regression analysis of the UV-Vis and NMR data without assumptions made in the Benesi-Hildebrand method. In this case, solving equation S2 leads to:

$$C_{com} = (C^o_A + C^o_D + 1/K_{eff}) +/- (((C^o_A + C^o_D + 1/K_{eff})^2 - 4C^o_A C^o_D)^{0.5}\}/2 \quad \text{(S6)}$$

So, changes in the UV-Vis absorption intensity and shift of the proton signal can be expressed as:

$$\Delta Abs = \varepsilon l \times C_{com} = \varepsilon l \times \{(C^o_A + C^o_D + 1/K_{eff}) - ((C^o_A + C^o_D + 1/K_{eff})^2 - 4C^o_A C^o_D)^{0.5}\}/2 \quad \text{(S7)}$$

$$\Delta\delta = \Delta\delta_\infty C_{com}/C^o_D = (\Delta\delta_\infty/C^o_D) \times \{(C^o_A + C^o_D + 1/K_{eff}) - ((C^o_A + C^o_D + 1/K_{eff})^2 - 4C^o_A C^o_D)^{0.5}\}/2 \quad \text{(S8)}$$

where ε and l are extinction coefficient of the complex and the length of the cell which was used in the UV-Vis measurements, and $\Delta\delta_\infty = \delta_\infty - \delta_0$ is the difference between the ppm of the CHX_3 proton in the presence of the infinite concentration of anion, δ_∞ (i.e. when all CHX_3 molecules are bonded to anions) and that of the separate CHX_3, δ_0. The fitting of the results of the UV-Vis titrations to eqs S7 (with ε and K_{UV}^{eff} as the adjustable parameters) using the Origin Pro 2016 are illustrated in Figures S1D-S6D. They produced values of K_{UV}^{eff} and ε in Table S1. (These values were consistent with those obtained via the Benesi-Hildebrandt treatment). The fitting of the results of NMR experiments (with K_{NMR}^{eff} and $\Delta\delta_\infty$ as adjustable parameters) are illustrated in Figures S9 – S11. They produced the values of K_{NMR}^{eff} and $\Delta\delta_\infty$ in Table S1.

The spectral and computational data indicated, however, that interaction of trihalomethanes with nucleophile A^- resulted in formation of both XB and HB complexes. These processes are characterized by equilibria constants K_{XB} and K_{HB}, respectively (eqs S9 and S10):

$$CHX_3 + A^- \overset{K_{XB}}{\rightleftharpoons} [X_2HC\text{-}X\bullet\bullet\bullet A^-] \qquad (S9)$$

$$CHX_3 + A^- \overset{K_{HB}}{\rightleftharpoons} [X_3C\text{-}H\bullet\bullet\bullet A^-] \qquad (S10)$$

Analysis of the experimental data pointed out that interaction of trihalomethanes with anions produces under conditions of experiments predominantly 1:1 complexes (either XB or HB).[4] Their formation constants of the latter are expressed as:

$$K_{XB} = C_{XB} / ((C^o_D - C_{XB} - C_{HB})(C^o_A - C_{XB} - C_{HB})) \qquad (S11)$$

$$K_{HB} = C_{HB} / ((C^o_D - C_{XB} - C_{HB})(C^o_A - C_{XB} - C_{HB})) \qquad (S12)$$

where C_{XB} and C_{HB} are equilibria concentrations of the XB and HB complexes. Eqs S11 and S12 can be rearranged as:

$$K_{XB}((C^o_D - C_{XB} - C_{HB})(C^o_A - C_{XB} - C_{HB})) = C_{XB} \qquad (S13)$$

$$K_{HB}((C^o_D - C_{XB} - C_{HB})(C^o_A - C_{XB} - C_{HB})) = C_{HB} \qquad (S14)$$

Thus

$$(C^o_D - C_{XB} - C_{HB})(C^o_A - C_{XB} - C_{HB}) = C_{XB}/K_{XB} \qquad (S15)$$

$$(C^o_D - C_{XB} - C_{HB})(C^o_A - C_{XB} - C_{HB}) = C_{HB}/K_{HB} \qquad (S16)$$

Or

$$C_{HB}/K_{HB} = C_{XB}/K_{XB} \qquad (S17)$$

$$C_{XB} = K_{XB} C_{HB} / K_{HB} \qquad (S18)$$

[4] This conclusion is based on the observation that the Jobs plot (for both CHI_3 in the current work and $CHBr_3$ in the reported earlier data) shows the formation of 1:1 complex. Apparently, polarization of the CHX_3 molecule hinders the binding of the second anion (and this applies to both modes of interaction). Moreover, the fitting of the experimental data using the model in which XB and HB modes do not affect each other, i.e. $C_{XB} = K_{XB}\times(C^o_D - C_{XB})(C^o_A - C_{XB})$ and $C_{HB} = K_{HB}\times(C^o_D - C_{HB})(C^o_A - C_{HB})$ either failed to converge or produced unsatisfactory results (see Figure S12). Finally, the calculated free energies of formation of the triple $[A^-...HCX_3...A^-]$ complexes (in which one anion is XB bonded and another is HB bonded to the same CHX_3 molecule) were ~6 kcal/mol more positive than that of the XB or HB dyads. So, the ratio of concentrations of triple to double complexes $C_T/C_D = (K_T\times C_D\times C_A^2)/(K_D\times C_D\times C_A) = \exp(-\Delta\Delta G/RT)\times C_A$ (where K_T is a formation constant of the triple complex, and K_D is a formation constant of the XB or HB complex, and $\Delta\Delta G$ is the difference between free energies of their formations). Since $C_A < 1$ M and $\exp(-\Delta\Delta G/RT) \approx \exp(-6/0.6) \approx 4.5\times10^{-5}$, the $C_T < C_D \times 10^{-4}$ and can thus formation of triple complxes can be neglected.

$$C_{HB} = K_{HB}C_{XB}/K_{XB} \quad \text{(S19)}$$

substitution of C_{HB} in eq S15 (using eq S19) and rearrangements leads to the quadratic equation:

$$(C^o_D - C_{XB}(1+ K_{HB}/K_{XB}))(C^o_A - C_{XB}(1+ K_{HB}/K_{XB})) - C_{XB}/K_{XB} = 0 \quad \text{(S20)}$$

$$C^o_A C^o_D/(1 + K_{HB}/K_{XB}) - C_{XB}(C^o_A + C^o_D + 1/(K_{XB}+K_{HB})) + C_{XB}^2(1 + K_{HB}/K_{XB}) = 0 \quad \text{(S21)}$$

Thus:

$$C_{XB} = \{(C^o_A+C^o_D+1/(K_{XB}+K_{HB})) - ((C^o_A+C^o_D+1/(K_{XB}+K_{HB}))^2 - 4C^o_A C^o_D)^{0.5}\}/(2(1+K_{HB}/K_{XB})) \quad \text{(S22)}$$

In a similar way:

$$C_{HB} = \{(C^o_A+C^o_D+1/(K_{XB}+K_{HB})) - ((C^o_A+C^o_D+1/(K_{XB}+K_{HB}))^2 - 4C^o_A C^o_D)^{0.5}\}/(2(1+K_{XB}/K_{HB})) \quad \text{(S23)}$$

As such, $\Delta Abs = \varepsilon l \times C_{XB} =$

$$= \varepsilon l \times \{(C^o_A+C^o_D+1/(K_{XB}+K_{HB})) - ((C^o_A+C^o_D+1/(K_{XB}+K_{HB}))^2 - 4C^o_A C^o_D)^{0.5}\}/(2(1+K_{HB}/K_{XB})) \quad \text{(S24)}$$

$$\Delta\delta = \Delta\delta_{XB}/C^o_D \times C_{XB} + \Delta\delta_{HB}/C^o_D \times C_{HB} =$$

$$= \Delta\delta_{XB}/C^o_D \times \{(C^o_A+C^o_D+1/(K_{XB}+K_{HB})) - ((C^o_A+C^o_D+1/(K_{XB}+K_{HB}))^2 - 4C^o_A C^o_D)^{0.5}\}/(2(1+K_{HB}/K_{XB}))$$

$$+ \Delta\delta_{HB}/C^o_D \times \{(C^o_A+C^o_D+1/(K_{XB}+K_{HB})) - ((C^o_A+C^o_D+1/(K_{XB}+K_{HB}))^2 - 4C^o_A C^o_D)^{0.5}\}/(2(1+K_{XB}/K_{HB})) \quad \text{(S25)}$$

Simultaneous fitting of the dependencies of ΔAbs and $\Delta\delta$ on concentration of A^- using eqs S24 and S25 (multivariable non-linear fitting option in Origin Pro 2016) are illustrated in Figures S13 – S19 (Table S4).[5] In these fitting, the concentration of anion $[A^-]$ was independent variable, values of ΔAbs and $\Delta\delta$ were two dependent variables, K_{HB}, K_{XB} and ε were adjustable parameters, and $\Delta\delta_{XB}$ and $\Delta\delta_{HB}$ (taken from computations) and concentration of CHX_3 were constant. Such fittings produced values of K_{XB} and K_{HB}.

It should be noted that the dependences of the values of ΔAbs and $\Delta\delta$ on concentration of anions in eqs S24 and S25 are similar to that in eqs S7 and S8 (although the K_{eff} in eqs S7 and S8 are replaced by combinations of K_{HB} and K_{XB} in eqs 21 and 22). This similarity explains the fact that the spectral data apparently could be fitted using eqs S7 and S8**.** However**,** the values of the formation constants of the dominant (XB or HB) complex resulting from such fitting may differ substantially from the correct value, and formation of the less stable complex can be overlooked.

[5] The simultaneous fitting of the dependencies of ΔAbs and $\Delta\delta$ on C^o_A (at constant C^o_D) with five adjustable parameters (K_{HB}, K_{XB}, $\Delta\delta_{XB}$, $\Delta\delta_{HB}$ and ε) produced unreliable results with the standard errors higher than 100%.

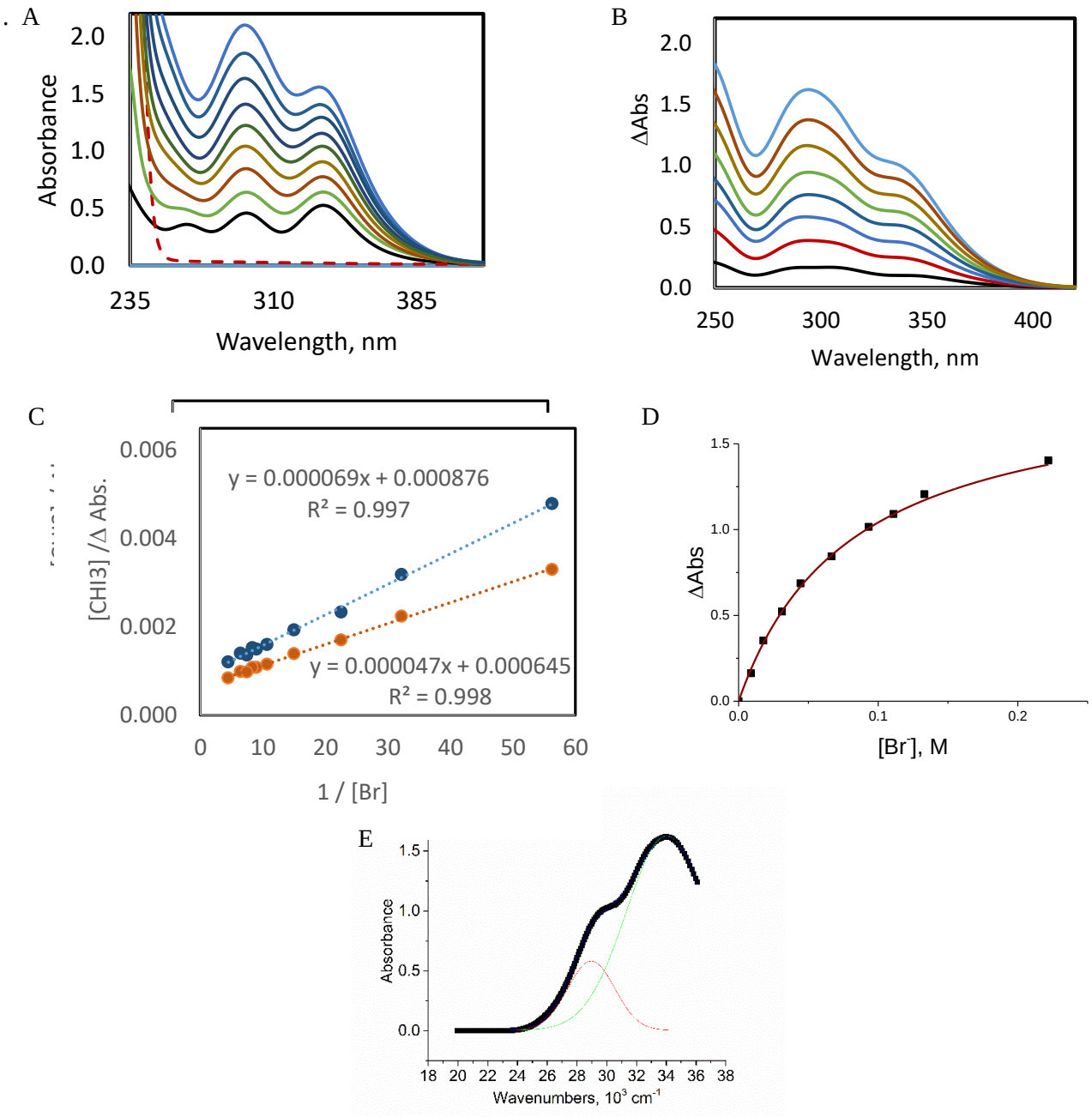

Figure S1. A) UV-Vis spectra of solutions with constants concentration of CHI_3 (1.1 mM) and various concentrations of Pr_4NBr salt in acetonitrile. The solid black line and dashed red line represent spectra of solutions of individual CHI_3 (1.1 mM) and Pr_4NBr (222 mM), respectively. Concentration of Pr_4NBr (solid lines, from bottom to top): 0 mM, 8.8 mM, 17.8 mM, 31.0 mM, 44.4 mM, 66.6 mM, 93.2 mM, 119.8 mM, and 133.1 mM. B) Differential absorption spectra obtained by subtraction of the absorption of components from the spectra of the mixtures representing absorption spectra of the [CHI_3, Br^-] complexes. C) Benesi-Hildebrand treatment of absorption data. D) Fitting of the ΔAbs to eq S7 (i.e. assuming one complex formation). E) Deconvolution of the absorption of the [CHI_3, Br^-] complex into Gaussian components.

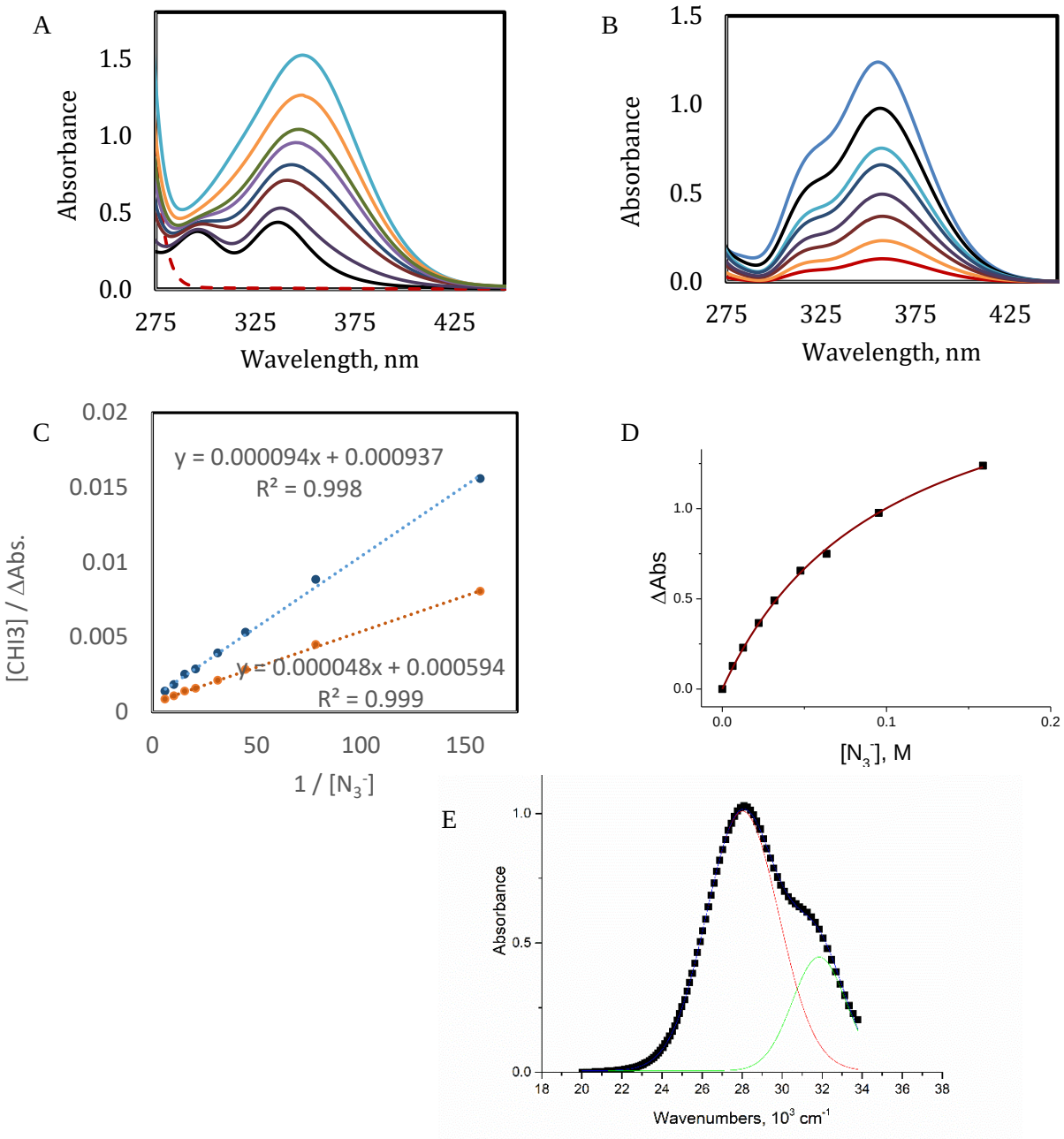

Figure S2. A) UV-Vis spectra of solutions with constants concentration of CHI_3 (1.1 mM) and various concentrations of Pr_4NN_3 salt in acetonitrile. The solid black line and dashed red line represent spectra of solutions of individual CHI_3 (1.1 mM) and Pr_4NBr (249 mM), respectively. Concentration of Pr_4NN_3 (solid lines, from bottom to top): 0 mM, 6.4 mM, 22.2 mM, 31.8 mM. 47.6 mM, 63.5 mM, 95.3 mM, and 158.8 mM. B) Differential absorption spectra obtained by subtraction of the absorption of components from the spectra of the mixtures representing absorption spectra of the [CHI_3, N_3^-] complexes. C) Benesi-Hildebrand treatment of absorption data. D) Fitting of the ΔAbs to eq S7 (i.e. assuming one complex formation). E) Deconvolution of the absorption of the [CHI_3, N_3^-] complex into Gaussian components.

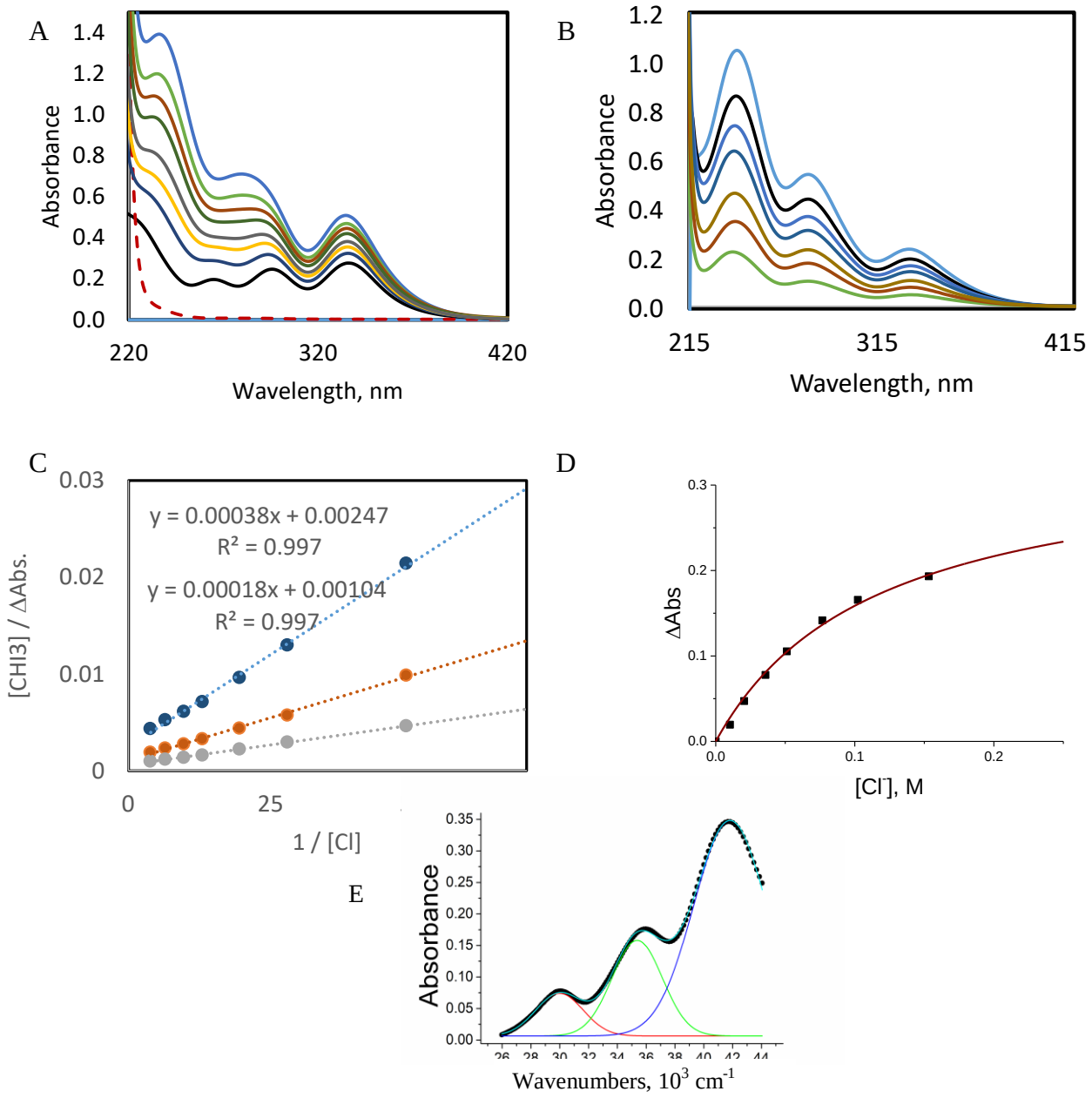

Figure S3. A) UV-Vis spectra of solutions with constants concentration of CHI_3 (1.1 mM) and various concentrations of Pr_4NCl salt in acetonitrile. The solid black line and dashed red line represent spectra of solutions of individual CHI_3 (1.1 mM) and Pr_4NCl (255 mM), respectively. Concentration of Cl^- (solid lines, from bottom to top): 0 mM, 10 mM, 20 mM, 36 mM, 51 mM, 77 mM, 102 mM, 153 mM, and 255 mM. B) Differential absorption spectra obtained by subtraction of the absorption of components from the spectra of the mixtures representing absorption spectra of the [CHI_3, Cl^-] complexes. C) Benesi-Hildebrand treatment of absorption data. D) Fitting of the ΔAbs to eq S7 (i.e. assuming one complex formation). E) Deconvolution of the absorption of the [CHI_3, Cl^-] complex into Gaussian components.

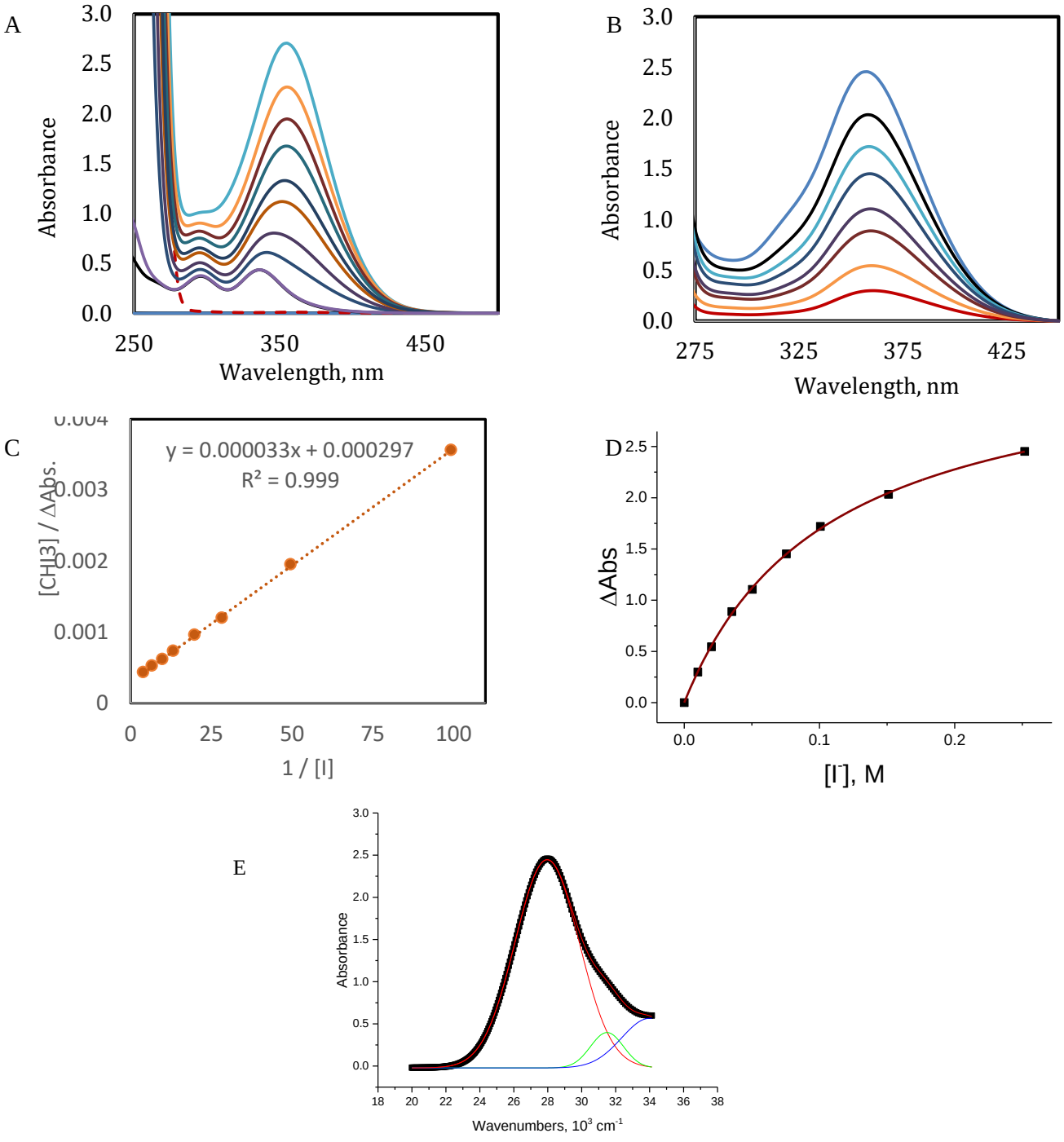

Figure S4. A) UV-Vis spectra of solutions with constants concentration of CHI_3 (1.1 mM) and various concentrations of Pr_4NI salt in acetonitrile. The solid black line and dashed red line represent spectra of solutions of individual CHI_3 (1.1 mM) and Pr_4NI (252 mM), respectively. Concentration of I^- (solid lines, from bottom to top): 0 mM, 10.1 mM, 35.2 mM, 50.4 M, 75.5 mM. 100.7 mM, 151.1 mM, and 251.8 mM. B) Differential absorption spectra obtained by subtraction of the absorption of components from the spectra of the mixtures representing absorption spectra of the [CHI_3, I^-] complexes. C) Benesi-Hildebrand treatment of absorption data. D) Fitting of the ΔAbs to eq S7 (i.e. assuming one complex formation). E) Deconvolution of the absorption of the [CHI_3, I^-] complex into Gaussian components.

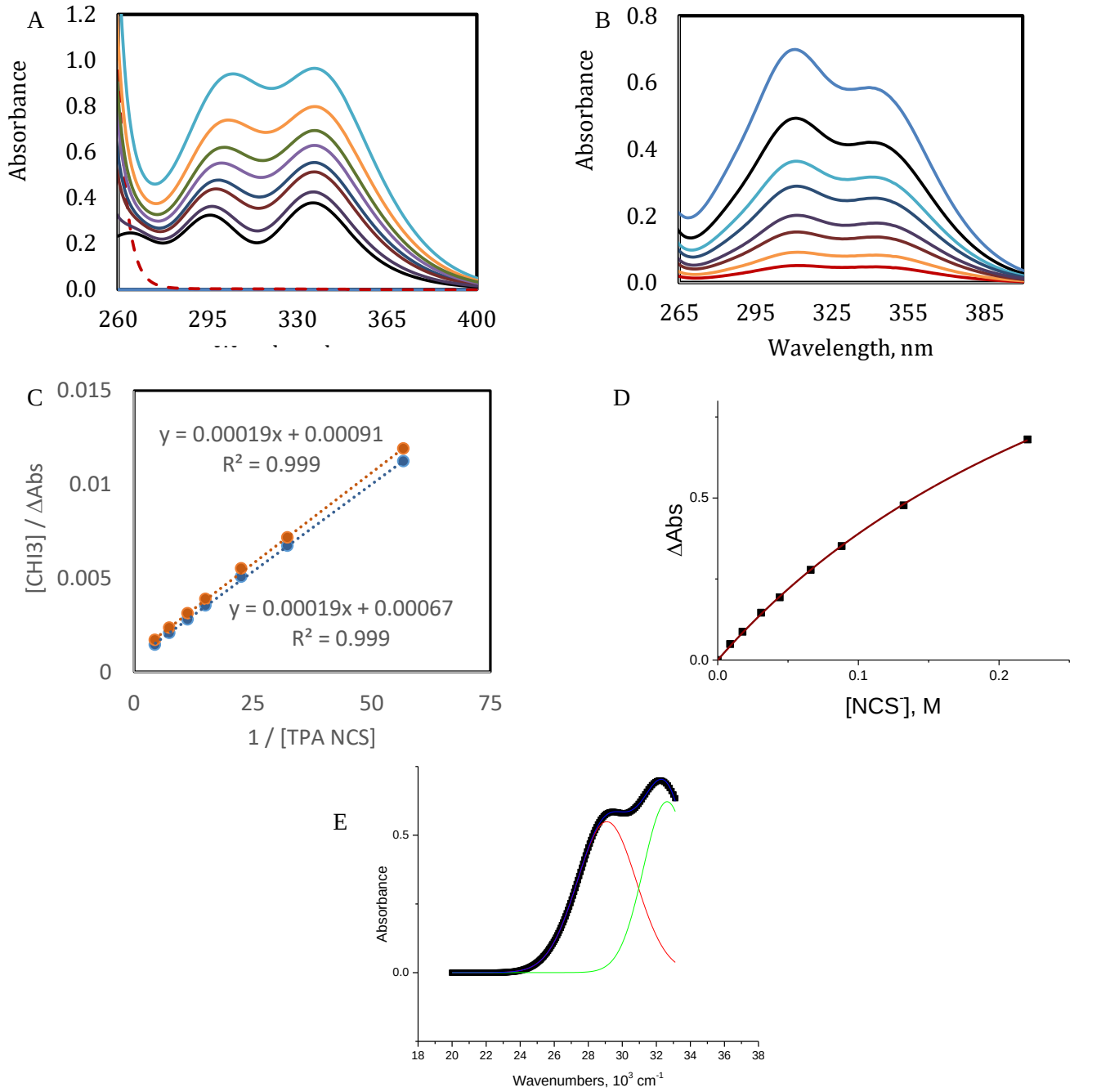

Figure S5. A) UV-Vis spectra of solutions with constants concentration of CHI_3 (1.1 mM) and various concentrations of Pr_4NNCS salt in acetonitrile. The solid black line and dashed red line represent spectra of solutions of individual CHI_3 (1.1 mM) and Pr_4NNCS (255 mM), respectively. Concentration of NCS^- (solid lines, from bottom to top): 0 mM, 8.8 mM, 17.6 mM, 30.8 mM, 44.1 mM. 66.1 mM, 132.2 mM, and 220.3 mM. B) Differential absorption spectra obtained by subtraction of the absorption of components from the spectra of the mixtures representing absorption spectra of the [CHI_3, NCS^-] complexes. C) Benesi-Hildebrand treatment of absorption data. D) Fitting of the ΔAbs to eq S7 (i.e. assuming one complex formation). E) Deconvolution of the absorption of the [CHI_3, NCS^-] complex into Gaussian components.

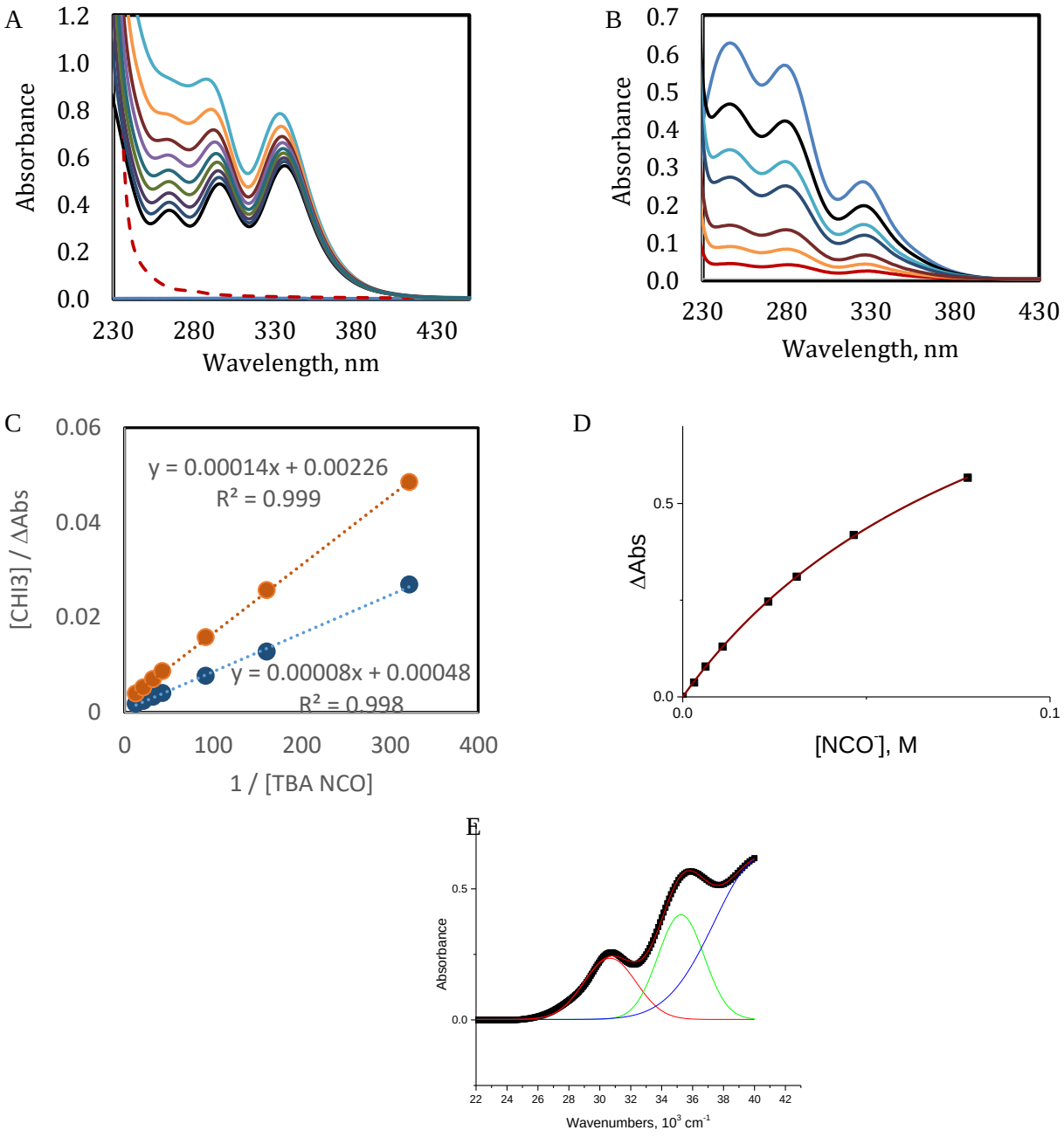

Figure S6. A) UV-Vis spectra of solutions with constants concentration of CHI_3 (1.1 mM) and various concentrations of Bu_4NNCO salt in acetonitrile. The solid black line and dashed red line represent spectra of solutions of individual CHI_3 (1.1 mM) and Bu_4NNCO (249 mM), respectively. Concentration of Bu_4NNCO (solid lines, from bottom to top): 0 mM, 3.1 mM, 6.2 mM, 10.9 mM. 15.5 mM, 23.3 mM, 3.1 mM, 46.6 mM and 77.6 mM. B) Differential absorption spectra obtained by subtraction of the absorption of components from the spectra of the mixtures representing absorption spectra of the [CHI_3, NCO^-] complexes. C) Benesi-Hildebrand treatment of absorption data. D) Fitting of the ΔAbs to eq S7 (i.e. assuming one complex formation). E) Deconvolution of the absorption of the [CHI_3, NCO^-] complex into Gaussian components.

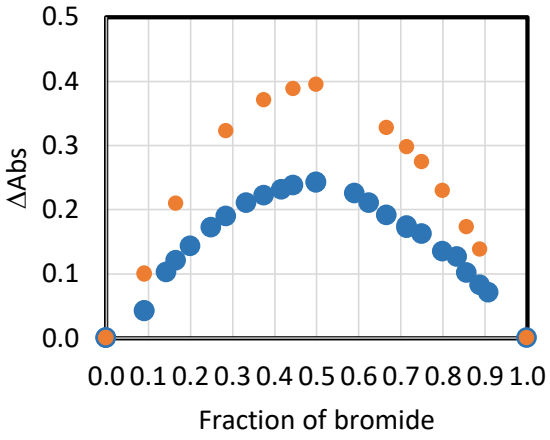

Figure S7. Job's plot: dependence of ΔAbs on the molar fraction of bromide for the solution containing CHI_3 and Br^- with constant sum of the concentration of components (20 mM) on fraction of Br^-(taken as a salt with Pr_4N^+ counter-ion). Blue and orange points show absorption measured at λ= 340 nm and λ= 296 nm, respectively.

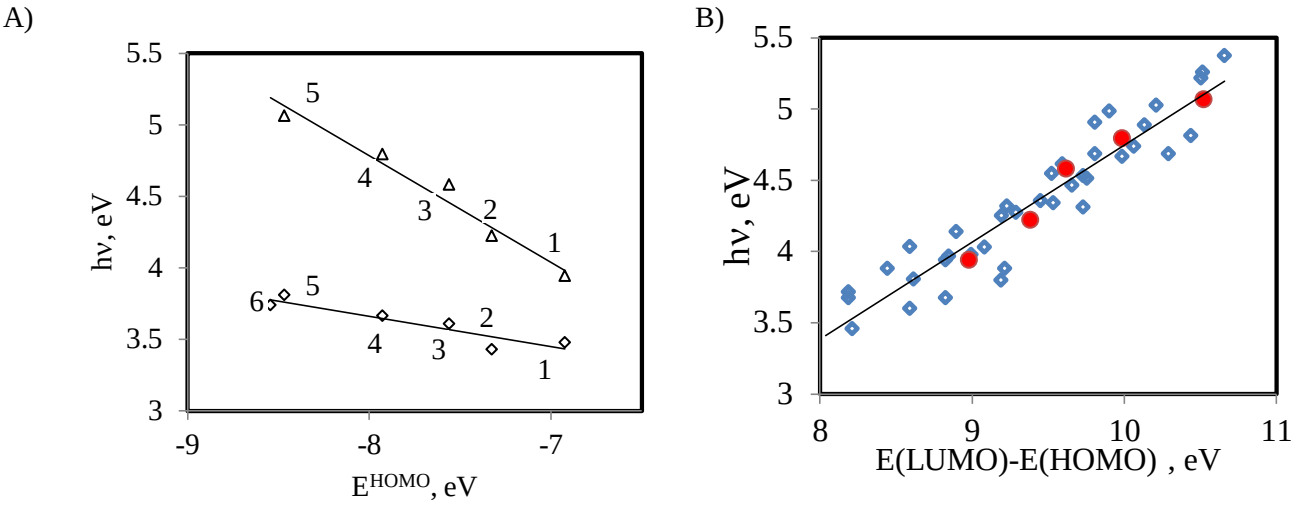

Figure S8.(A) Correlation between the energies of the absorption bands of the [CHX_3, A^-] complexes (CHI_3 (◊) or $CHBr_3$ (▵)) and the HOMO energies of A^- anions: N_3^- (1), I^- (2), NCS^- (3), Br^- (4), NCO^- (5), Cl^- (6)).
B) Mulliken correlation between the energies of the lowest-energy bands of the complexes of bromosubstituted electrophiles and anions, [R-Br, A^-] and the difference of their frontier orbital energies. Complexes of $CHBr_3$ are shown as red circles. HOMO/LUMO energies (from mp2/6-311G** /SCIPCM computations) and wavelengths are listed below (from refs 50- 52).

R-Br	E(LUMO)	Br^-	Cl^-	I^-	NCS^-	NCO^-	N_3^-
CBr_4	0.04652	292	265	345	315	274	338
$CHBr_3$	0.07564	259		294	275	245	315
CBr_3NO_2	0.04731	320	297			275	359
CBr_3CN	0.05593	285	262	327	308	266	320
CBr_3COOH	0.07215	289	238	300	273		297
$CFBr_3$	0.0613	269	247	312	287	254	308
CBr_3CONH_2	0.07255	249	236		286	258	300
$C_3Br_2F_6$	0.10039	231			265		278
CBr_3COCBr_3	0.0465	327	253		338	288	334
	E(HOMO)	-0.29131	-0.31396	-0.26925	-0.27785	-0.31113	-0.25444

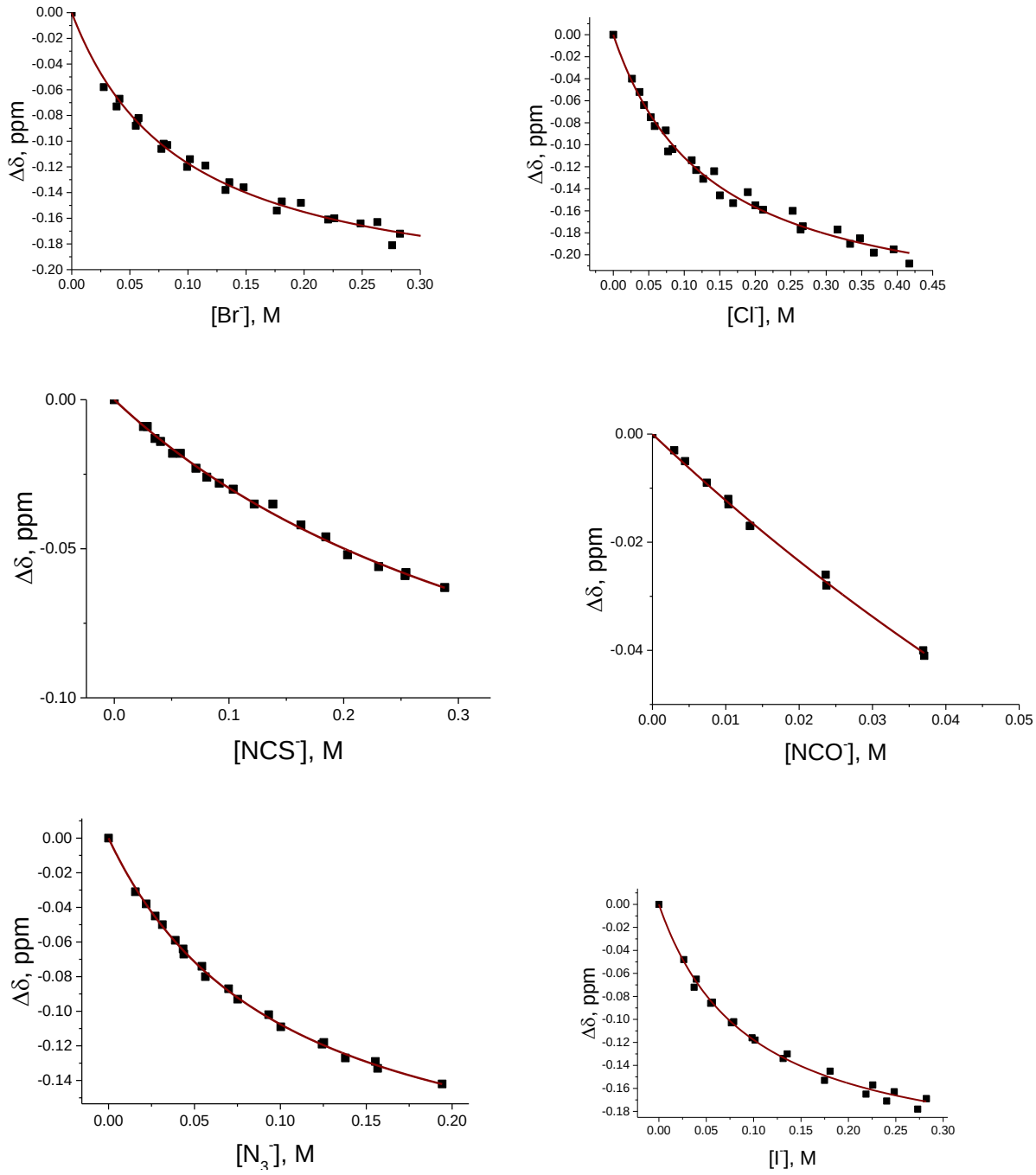

Figure S9. Results of the ^{1}H NMR measurements of solutions with constant concentration of CHI_3 (5.1 mM) and variable concentrations of with A^- anions (as indicated) (CD_3CN, 22^{o}C) and their fitting using eq S8. Note, the combined results of 2-3 independent series for each pair are shown; anions were taken as Pr_4NA salts.

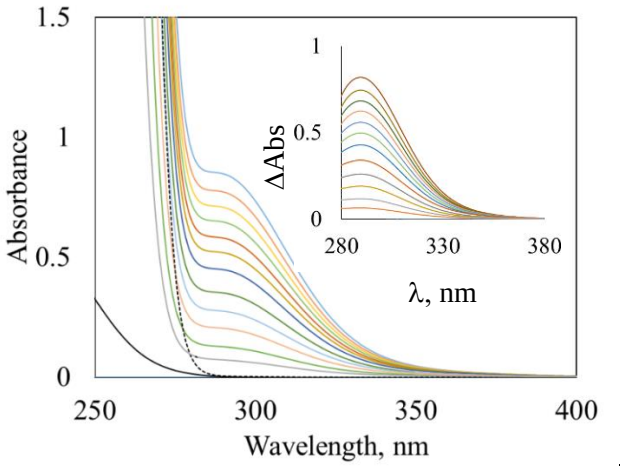

Figure S10. Spectra of solutions with constant concentration of $CHBr_3$ (5.0 mM) and various concentrations of Pr_4NI (solid lines from the bottom to the top: 0, 13.7, 27.4, 45.6, 63.9, 82.2, 110, 128, 146, 164, 183, 201 and 228 mM). Spectrum of the separate 200 mM solution of Pr_4NI is shown as a dashed line. Insert: Spectra obtained by subtraction of the absorption of components from the spectra of their mixtures.

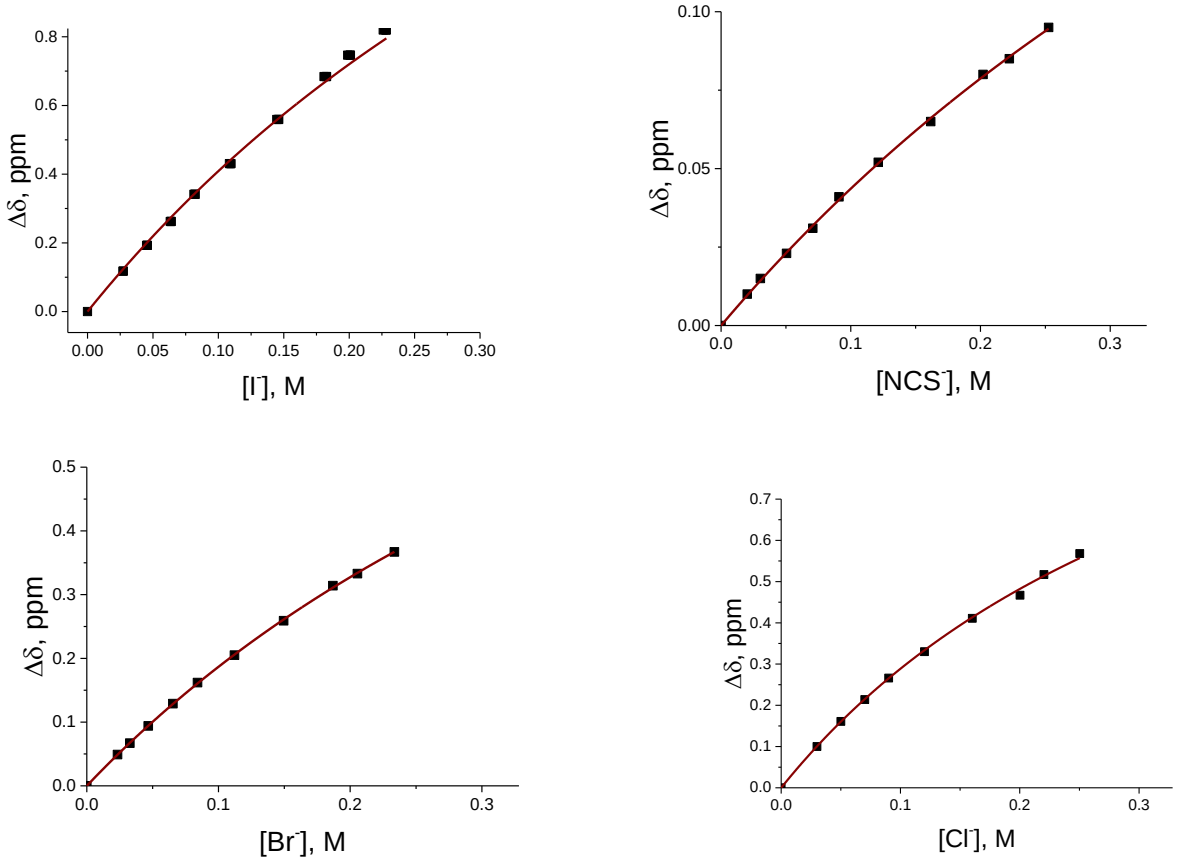

Figure S11. Results of the ^1H NMR measurements of solutions with constant concentration of $CHBr_3$ (5.0 mM) and variable concentrations of A^- anions (as indicated) (CD_3CN, 22°C) and their fitting using eq S8. Note, the combined results of 2-3 independent series for each pair are shown; anions were taken as Pr_4NA salts.

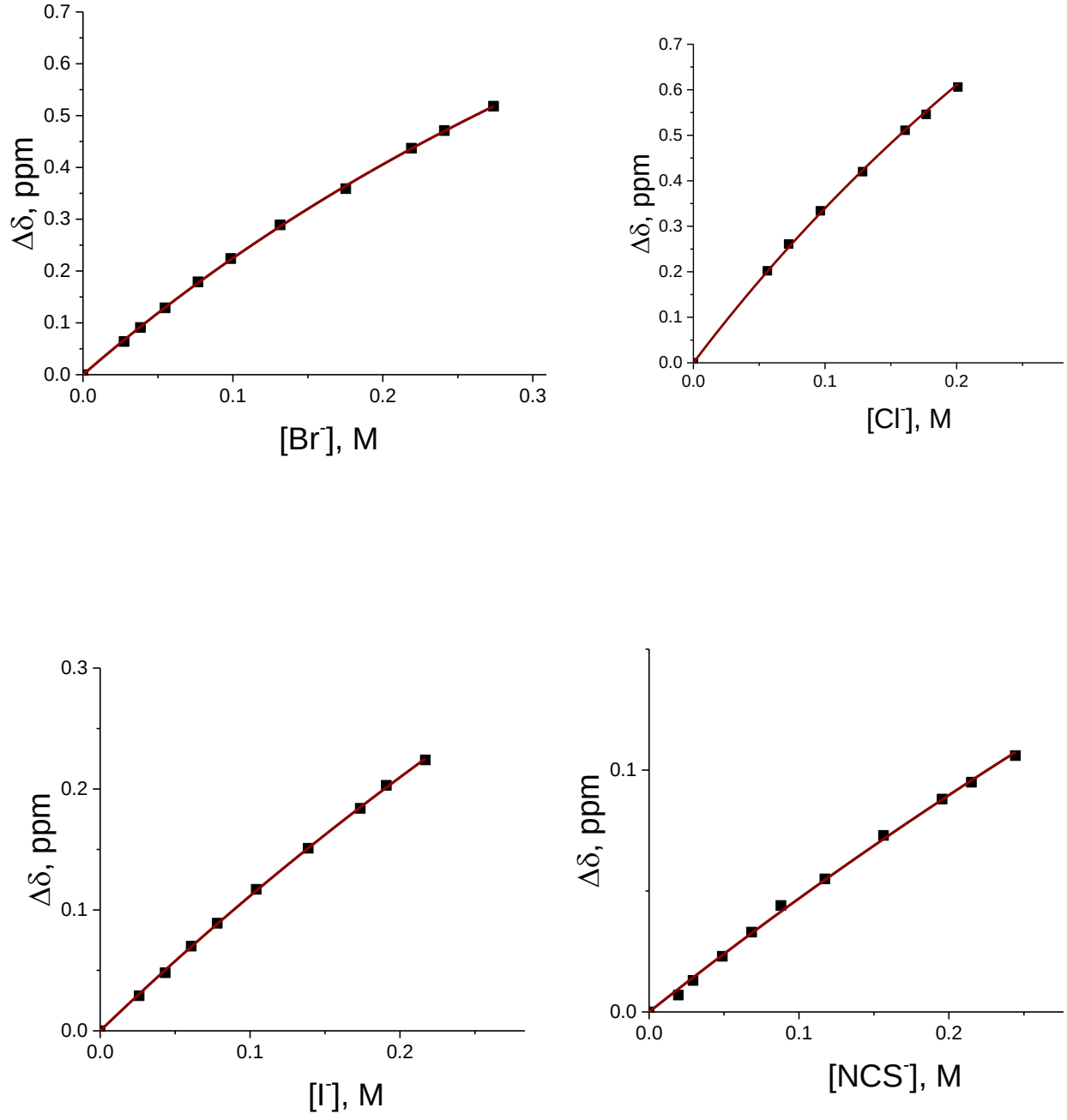

Figure S12. Results of the ^{1}H NMR measurements of solutions with constant concentration of $CHCl_3$ (5.1 mM) and variable concentrations of A^- anions (as indicated) (CD_3CN, 22^{o}C) and their fitting using eq S8. Note, the combined results of 2-3 independent series for each pair are shown; anions were taken as Pr_4NA salts.

Table S1. Effective formation constants of [CHX_3, A^-] complexes.[a]

CHX_3	A^{-b}	K_{UV}^{eff}, M^{-1}	$K_{NMR}^{eff,}$ M^{-1}
CHI_3	I^-	10.5±0.9	10.9±0.5
	Br^-	11.7±1.0	10.7±1.1
	Cl^-	9.2±0.6	7.0±0.5
	NCS^-	2.4±0.5	2.3±0.4
	NCO^-	9.2±2.1	5.1±0.4
	N_3^-	10.7±1.3	9.9±0.8
$CHBr_3$	I^-	0.4[c]	1.0±0.1
	Br^-	0.33[d]	1.4±0.3
	Cl^-	-	2.4±0.3
	NCS^-	~0.3[e]	1.2±0.1
	NCO^-	~0.1[e]	-
	N_3^-	~0.4[e]	-
$CHCl_3$	I^-	-	0.6±0.1
	Br^-	-	1.3±0.2
	Cl^-	-	1.6±0.2
	NCS^-	-	0.5±0.2

a) In CH_3CN, calculated (as in earlier studies) assuming that only one type of complex is formed in solutions. b) Taken as salts with Pr_4N^+ or Bu_4N^+ counter-ions. c) From ref. 51. b) From ref. 49. e) From ref. 50.

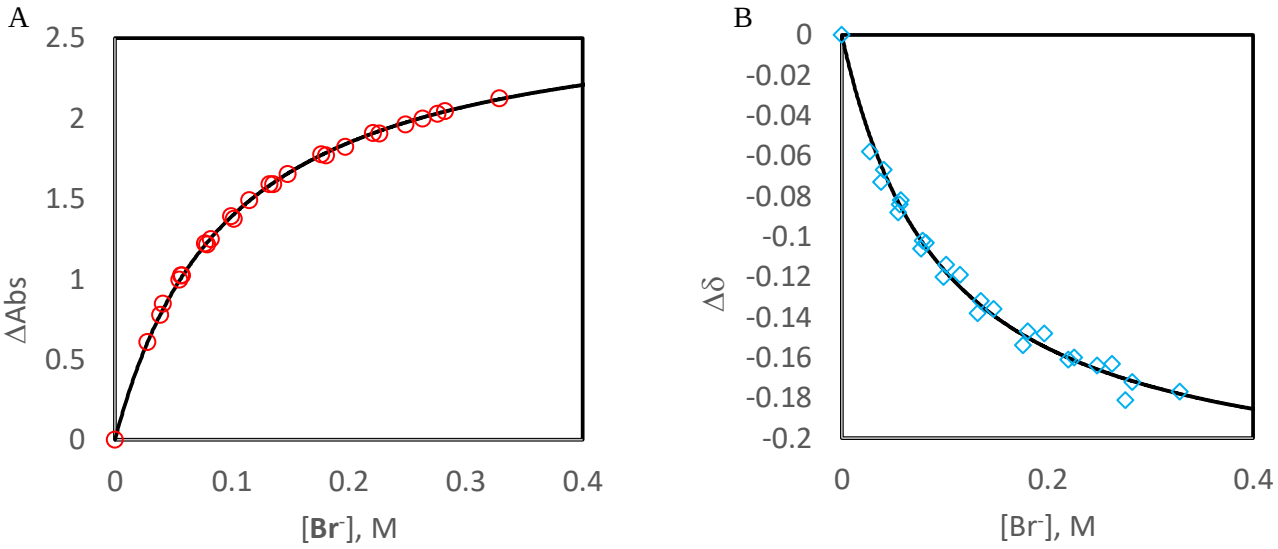

Results

	Value	Standard Error	t-Value	Prob>|t|
Kx	9.44972	0.10228	92.38868	0
Kh	1.18366	0.02208	53.59965	0
Sx	-0.54	0	--	--
Sh	2.25	0	--	--
εl	659.9113	2.71039	243.4748	0

Statistics

Number of Points	54
Degrees of Freedom	51
Reduced Chi-Sqr	1.31E-04
Residual Sum of Squares	6.68E-03
R-Square(COD)	0.99984
Adj. R-Square	0.99983

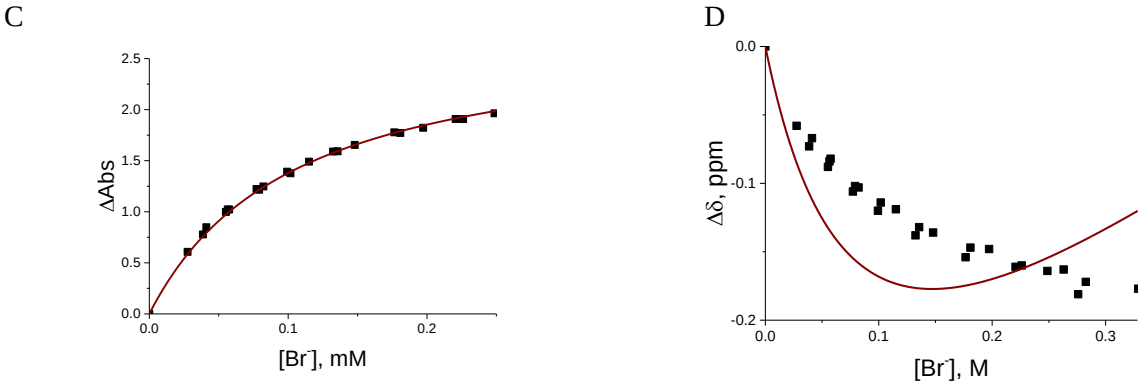

Figure S13. Results of the UV-Vis (A) and ^{1}H NMR (B) measurements of solutions with constant concentration of CHI_3 (5.1 mM) and variable concentrations of Pr_4NBr and their simultaneous multivariable fitting to eqs S24 and S25. Note that the combined results of 3 independent series are shown. The table below the figures shows results of the fitting and their statistical analysis which were copied from the output of the fitting (Origin 2016). Figures C and D illustrate *inadequacy* of the fitting assuming that formation of XB do not affect that of HB complexes, and vice versa (i.e., $K_{XB}= C_{XB} / ((C^o_D - C_{XB})(C^o_A - C_{XB}))$ and $K_{HB}= C_{HB} / ((C^o_D - C_{HB})(C^o_A - C_{HB}))$.

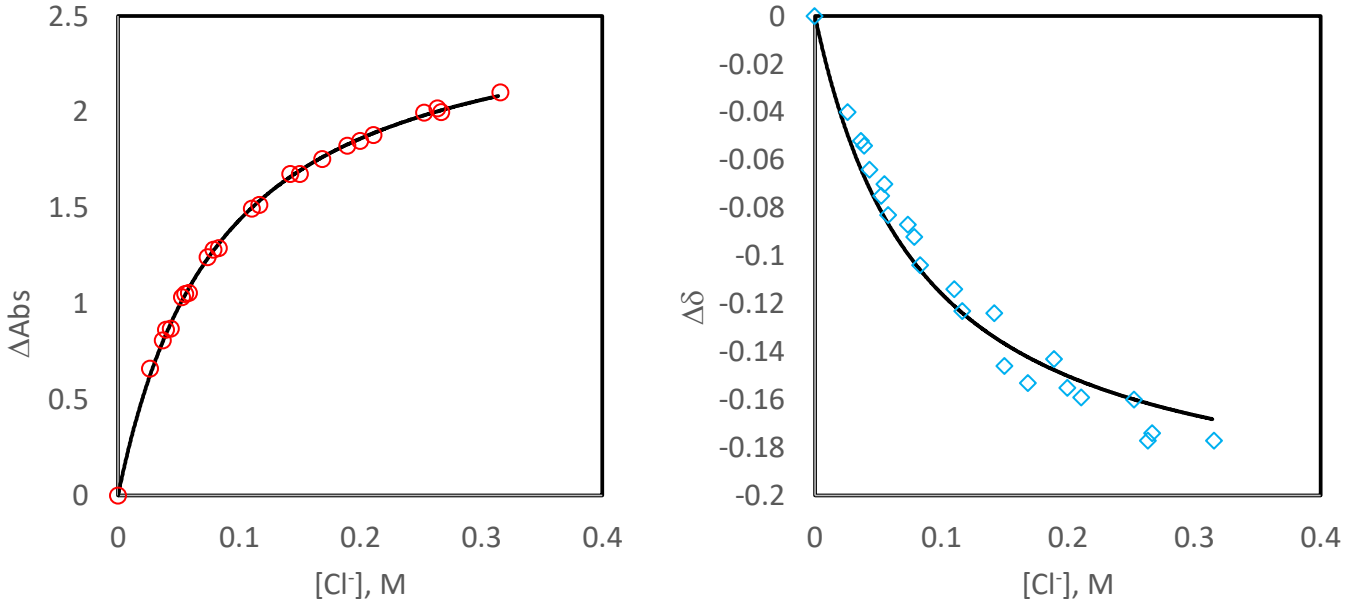

Results

	Value	Standard Error	t-Value	Prob>|t|
Kx	10.40763	0.14838	70.14397	0
Kh	1.9523	0.04152	47.01999	0
Sx	-0.61	0	--	--
Sh	1.91	0	--	--
εl	669.05244	3.6798	181.8178	0

Statistics

Number of Points	48
Degrees of Freedom	45
Reduced Chi-Sqr	1.88E-04
Residual Sum of Squares	0.00845
R-Square(COD)	0.99975
Adj. R-Square	0.99974

Figure S14. Results of the UV-Vis (A) and ^{1}H NMR (B) measurements of solutions with constant concentration of CHI_3 (5.1 mM) and variable concentrations of Pr_4NCl and their simultaneous multivariable fitting to eqs S24 and S25. (Note, the combined results of 3 independent series). The tables below the figures shows results of the fitting and their statistical analysis which were copied from the output of the fitting (Origin 2016).

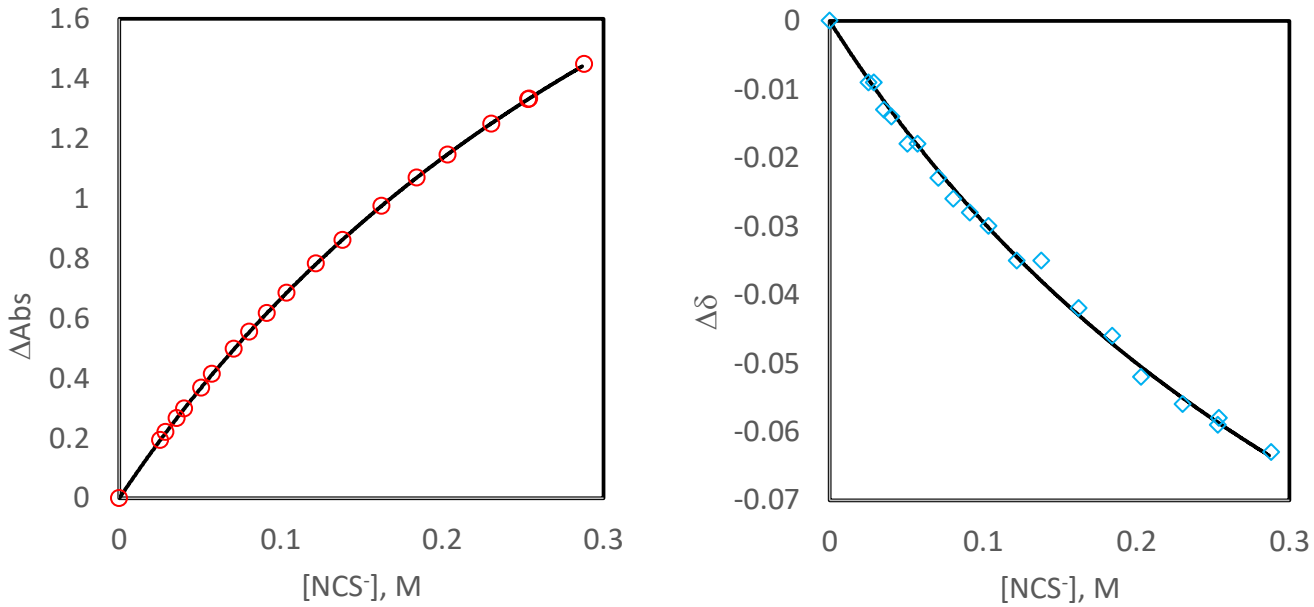

Results:

	Value	Standard Error	t-Value	Prob>|t|
Kx	1.6953	0.00607	279.2472	0
Kh	0.43096	0.00287	149.982	0
Sx	-0.46	0	--	--
Sh	0.98	0	--	--
ε*l*	1028.01652	2.59811	395.6784	0

Statistics

Number of Points	40
Degrees of Freedom	37
Reduced Chi-Sqr	1.25E-06
Residual Sum of Squares	4.63E-05
R-Square(COD)	1
Adj. R-Square	0.99999

Figure S15. Results of the UV-Vis (A) and ^{1}H NMR (B) measurements of solutions with constant concentration of CHI_3 (5.1 mM) and variable concentrations of Pr_4NNCS and their simultaneous multivariable fitting to eqs S24 and S25. (Note, the combined results of 3 independent series). The tables below the figures shows results of the fitting and their statistical analysis which were copied from the output of the fitting (Origin 2016).

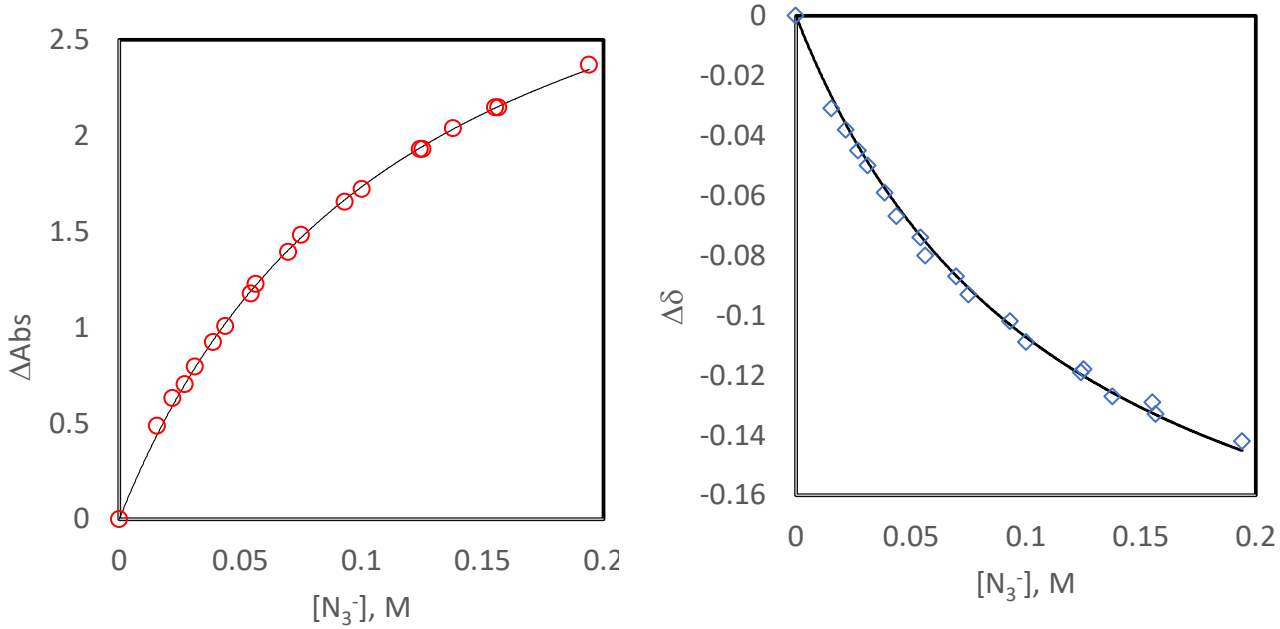

	Value	Standard Error	t-Value	Prob>|t|
Kx	7.63682	0.12909	59.1589	0
Kh	1.22041	0.035	34.87078	0
Sx	-0.64	0	--	--
Sh	2.33	0	--	--
E	961.3116	8.38307	114.673	0

Number of Points	38
Degrees of Freedom	35
Reduced Chi-Sqr	1.65E-04
Residual Sum of Squares	0.00579
R-Square(COD)	0.99979
Adj. R-Square	0.99978

Figure S16. Results of the UV-Vis (A) and ^{1}H NMR (B) measurements of solutions with constant concentration of CHI_3 (5.1 mM) and variable concentrations of Pr_4NN_3 and their simultaneous multivariable fitting to eqs S24 and S25. (Note, the combined results of 3 independent series). The tables below the figures shows results of the fitting and their statistical analysis which were copied from the output of the fitting (Origin 2016).

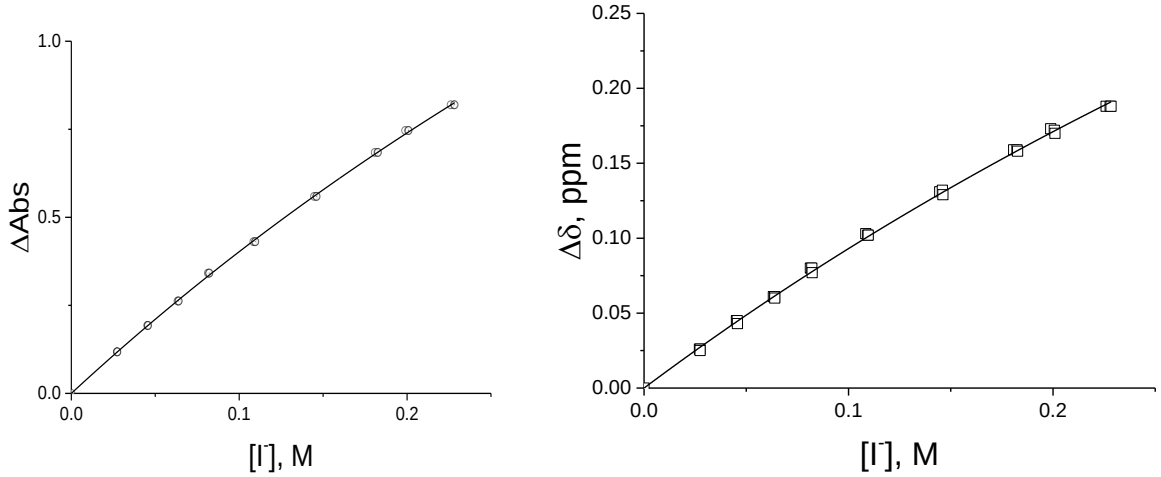

Results

	Value	Standard Error	t-Value	Prob>|t|	Dependency
Kx	0.36855	0.02599	14.18103	0	0.99964
Kh	0.6032	0.00707	85.29423	0	0.81803
Sx	-0.28	0	--	--	0
Sh	1.87	0	--	--	0
εl	2580.056	169.2578	15.24335	0	0.99963

Statistics

Number of Points	56
Degrees of Freedom	53
Reduced Chi-Sqr	1.16E-05
Residual Sum of Squares	6.13E-04
R-Square(COD)	0.99982
Adj. R-Square	0.99982

Figure S17. Results of the UV-Vis (A) and ^{1}H NMR (B) measurements of solutions with constant concentration of $CHBr_3$ (5.0 mM) and variable concentrations of Pr_4NI and their simultaneous multivariable fitting to eqs S24 and S25. (Note, the combined results of 2 independent series). The tables below the figures shows results of the fitting and their statistical analysis which were copied from the output of the fitting (Origin 2016).

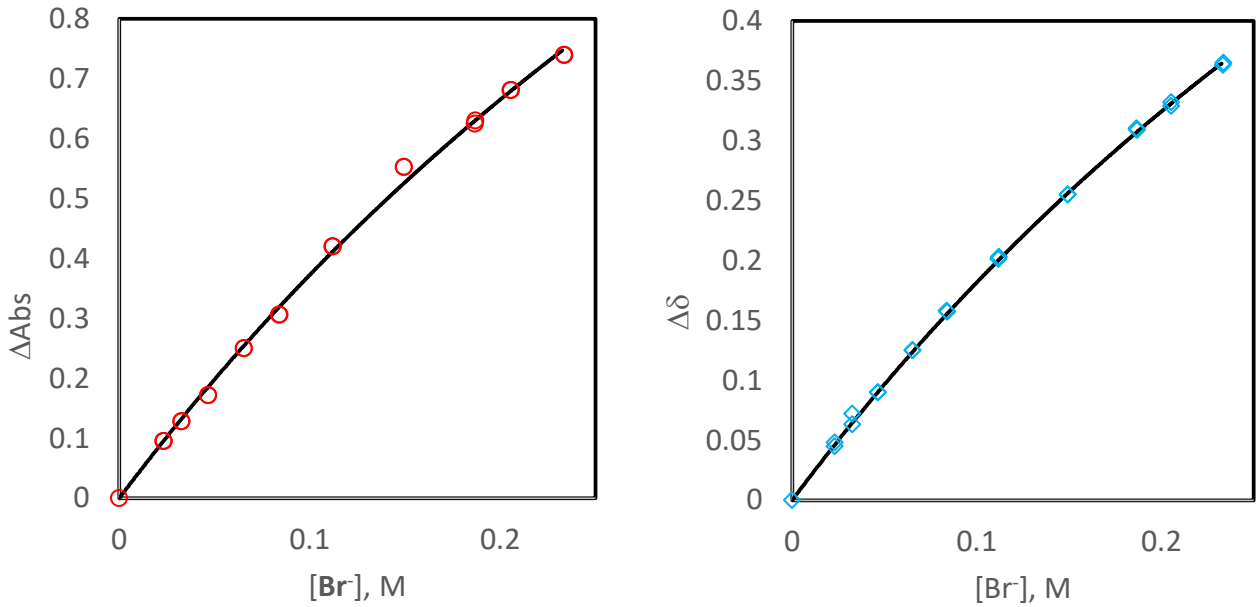

Results

	Value	Standard Error	t-Value	Prob>|t|
Kx	0.51888	0.08104	6.40309	1.43E-07
Kh	0.86927	0.02244	38.73442	0
Sx	-0.31	0	--	--
Sh	2.58	0	--	--
εl	1443.278	204.2232	7.06716	1.73E-08

Statistics

Number of Points	42
Degrees of Freedom	39
Reduced Chi-Sqr	7.11E-05
Residual Sum of Squares	2.77E-03
R-Square(COD)	0.99851
Adj. R-Square	0.99843

Figure S18. Results of the UV-Vis (A) and ^{1}H NMR (B) measurements of solutions with constant concentration of $CHBr_3$ (5.0 mM) and variable concentrations of Pr_4NBr and their simultaneous multivariable fitting to eqs S24 and S25. (Note, the combined results of 2 independent series). The tables below the figures shows results of the fitting and their statistical analysis which were copied from the output of the fitting (Origin 2016). Br

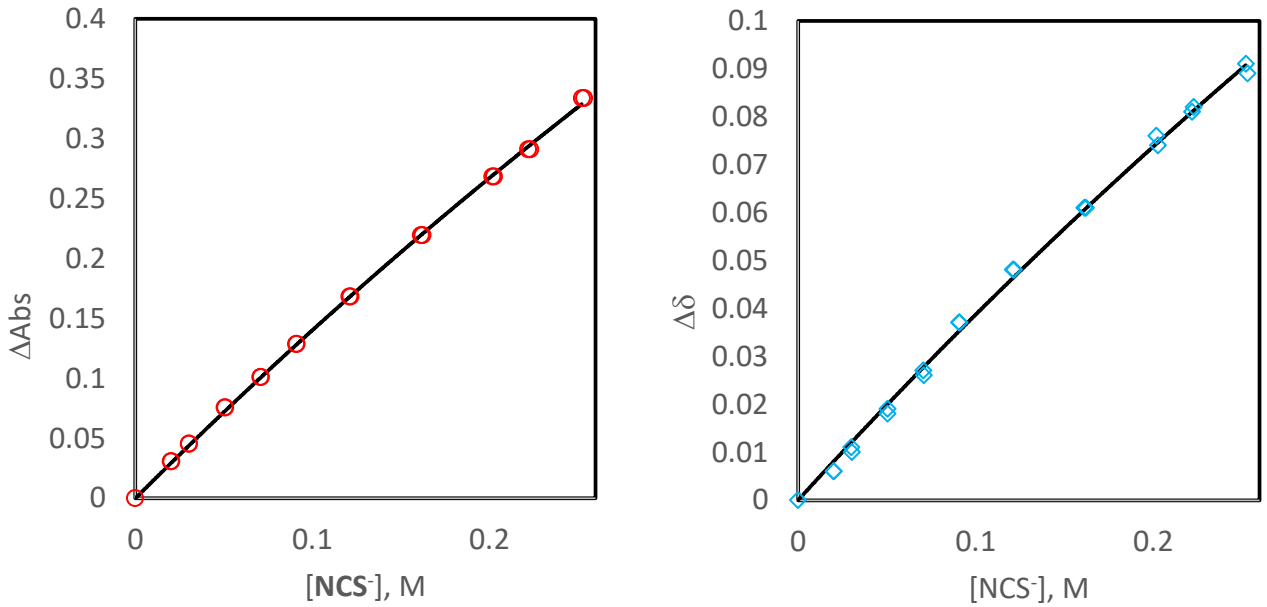

Results

	Value	Standard Error	t-Value	Prob>|t|	Dependency
Kx	0.09234	0.03277	2.818	0.00755	0.99996
Kh	0.43277	0.01081	40.04458	0	0.91109
Sx	-0.22	0	--	--	0
Sh	0.99	0	--	--	0
ε*l*	3202.691	1111.362	2.88177	0.0064	0.99996

Statistics

Number of Points	42
Degrees of Freedom	39
Reduced Chi-Sqr	3.30E-06
Residual Sum of Squares	1.29E-04
R-Square(COD)	0.99967
Adj. R-Square	0.99965

Figure S19. Results of the UV-Vis (A) and ^{1}H NMR (B) measurements of solutions with constant concentration of $CHBr_3$ (5.0 mM) and variable concentrations of Pr_4NNCS and their simultaneous multivariable fitting to eqs S24 and S25. (Note, the combined results of 2 independent series). The tables below the figures shows results of the fitting and their statistical analysis which were copied from the output of the fitting (Origin 2016).

Comparison of the simultaneous and separate fittings of the UV-Vis and NMR data

Since analysis of the equilibria in the solutions containing CHX_3 and anions produced expressions for ΔAbs and Δδ which include K_{HB} and K_{XB} (eqs S24 and S25), we carried out separate fitting of the UV-Vis data measured for each pair using eq S24 and separate fitting of the NMR data using eq S25. Importantly, these fitting were based on the model which takes into account formation of both XB and HB complexes, and produce both K_{XB} and K_{HB} values (in contrast to the earlier studies, in which separate treatments of the UV-Vis and NMR data were done assuming formation of only one type of complex yielding K_{UV}^{eff} and K_{NMR}^{eff} values). The principal results of such fitting (K_H, K_X and their standard errors) are listed in Table S2.

Table S2. Comparison of the results of simultaneous and separate fitting of the UV-Vis and NMR data.

Pair		Values from simultaneous (multivariable) fitting		Values from fitting of NMR data only [a]		K(NMR)/ K(NMR+UV)[c]	Values from fitting of UV-Vis data only [a]	
		Value	Std Err	Value	Std Err		Value	Std Err
CHI_3/Br^-	K_{XB}	9.478	0.103	9.730	0.500	1.03	6.997	732
	K_{HB}	1.188	0.022	1.229	0.082	1.03	3.667	735
CHI_3/I^-	K_{XB}	7.688	0.064	9.454	0.423	1.23	10.107	160
	K_{HB}	1.125	0.031	1.512	0.093	1.34	-1.297	160
CHI_3/Cl^-	K_{XB}	11.014	0.163	6.850	0.502	1.38	7.760	1474
	K_{HB}	1.406	0.031	0.760	0.077	1.46	4.690	1479
CHI_3/NCS^-	K_{XB}	1.709	0.006	1.862	0.148	1.09	2.239	20
	K_{HB}	0.420	0.003	0.479	0.057	1.14	-0.109	20
CHI_3/N_3^-	K_{XB}	7.674	0.131	8.931	0.292	1.16	7.341	573
	K_{HB}	1.227	0.035	1.498	0.063	1.22	1.554	574
$CHBr_3/Br^-$	K_{XB}	0.517	0.081	0.596	0.049	1.15	1.501	610
	K_{HB}	0.868	0.022	0.889	0.013	1.02	-0.138	612
$CHBr_3/I^-$	K_{XB}	0.369	0.026	0.472	0.058	1.28	1.510	230
	K_{HB}	0.603	0.007	0.630	0.015	1.04	-0.550	231
$CHBr_3/NCS^-$	K_{XB}	0.091	0.044	0.087	0.126	0.96	0.835	587
	K_{HB}	0.436	0.014	0.434	0.040	1.00	-0.309	589
Average			0.049 (5.8%)[b]		0.159(15.3 %)[b]	1.16		549

a) Taking into account formation of both XB and HB complexes. b) Average relative error (i.e. $1/n\Sigma(error_i/value_i)$); c) Ratio of the value obtained from the separate fitting of the NMR data to that obtained from the simultaneous fitting of UV and NMR data.

The K_{HB} and K_{XB} constants resulting from the separate fitting of the NMR data are consistent (within the accuracy of experiments) with the values from the simultaneous fitting of the NMR and UV-Vis data. Yet, the errors from the separate fittings of the NMR data are, on average, about three times higher than that from the simultaneous fitting. Importantly, the calculated shifts of the NMR proton signal depend on the values of $\Delta\delta_{XB}$ and $\Delta\delta_{HB}$ taken from calculation. Since the simultaneous fittings yield the values, which describe variations of UV-Vis spectral data as well, the values resulting from such fitting are apparently more reliable. The values of ΔAbs are related only to the concentration of the XB complexes, and their separate three-parameters fitting using eq S24 produced large standard errors (though the accuracy of the UV-Vis measurements was somewhat higher

than that of the NMR measurements).[6] Overall, these data indicate that the combine fitting yield more reliable and accurate K_{HB} and K_{XB} values than the separate fittings. Thus, the conclusions of the paper are based on the results of only combined fittings.

It should be also noted that expression for the UV-Vis spectral changes $\Delta Abs = \varepsilon l \times C_{XB}$ (eq S24 or eq 8 in the text) neglect the spectral changes related to the formation of HB complexes (since spectra of the HB complexes are close to that of the separate molecules). If such changes are taken into account, ΔAbs is expressed as:

$$\Delta Abs = \Delta\varepsilon_{XB}\, l \times C_{XB} + \Delta\varepsilon_{HB}\, l \times C_{HB} \quad \text{(S26)}$$

where $\Delta\varepsilon_{XB}$ are $\Delta\varepsilon_{HB}$ differences between extinction coefficients of XB or HB bonded complexes and the separate CHX_3 molecules. Eq 26 could be rearranged as:

$$\Delta Abs = (\Delta\varepsilon_{XB} + \Delta\varepsilon_{HB}\, C_{HB}/ C_{XB}) \times l \times C_{XB} \quad \text{(S27)}$$

Taking into account eq S19, $C_{HB} = K_{HB}C_{XB}/K_{XB}$, leads to

$$\Delta Abs = (\Delta\varepsilon_{XB} + \Delta\varepsilon_{HB}\, K_{HB}/K_{XB}) \times l \times C_{XB} \quad \text{(S28)}$$

Accordingly, eS24 (eq 10 in the text) for fitting of UV-Vis data can be re-written as:

$$\Delta Abs = \varepsilon\, l \times \{(C^o_A + C^o_D + 1/(K_{XB}+K_{HB})) - ((C^o_A + C^o_D + 1/(K_{XB}+K_{HB}))^2 - 4C^o_A C^o_D)^{0.5}\}/(2(1+K_{HB}/K_{XB})) \quad \text{(S29)}$$

where $\varepsilon = \Delta\varepsilon_{XB} + \Delta\varepsilon_{HB}\, K_{HB}/K_{XB}$.

Equation S29 is identical to that in eq S24 (or eq 10), but with $\varepsilon = \Delta\varepsilon_{XB} + \Delta\varepsilon_{HB}\, K_{HB}/K_{XB}$. As such, fitting UV-Vis data using eq 29 would produce the same values of K_{HB} and K_{XB} as that obtained using eq 24. This analysis, however, shows that the extinction coefficients ε resulted from the separate fitting of UV-Vis data or combined fittings of NMR and UV-Vis data may differ more or less significantly from the extinction coefficients of the halogen-bonded complexes.

---

[6]Somewhat higher accuracy of the UV-Vis measurements is related to two factors, i.e. a) absolute errors in volumes of aliquots used in preparations of the solutions were the same, but the overall volume of the solution used for the UV-Vis measurements were typically twice as higher as that in the NMR; and b) since the ratio of the absolute changes in ΔAbs were larger than that of $\Delta\delta$ while the accuracy of the measurements of individual values of Abs and δ were similar.

The large standard errors in the last column of Table S2 d to two variable parameters (K_{XB}, K_{HB}) used for$\Delta\delta$ fittings via eq S25. The comparable fittings of the UV-Vis and NMR data (using, in both cases, two variable parameters, K_{XB} and K_{HB}, and fixed values of ε or $\Delta\delta_{XB}$ and $\Delta\delta_{HB}$) yield similar standard errors. For example, the two-parameter fitting of the UV-Vis data for CHI_3/I^- pair yielded $K_{XB} = 7.660 \pm 0.052$ and $K_{HB} = 1.110 \pm 0.049$, while comparable fitting of the NMR data yielded $K_{XB} = 9.954 \pm 0.423$ and $K_{HB} = 1.512 \pm 0.093$; and fitting of UV-Vis data for $CHBr_3/I^-$ pair yielded $K_{XB} = 0.362 \pm 0.002$ and $K_{HB} = 0.604 \pm 0.048$, while NMR data yielded: $K_{XB} = 0.472 \pm 0.058$ and $K_{HB} = 0.630 \pm 0.015$.

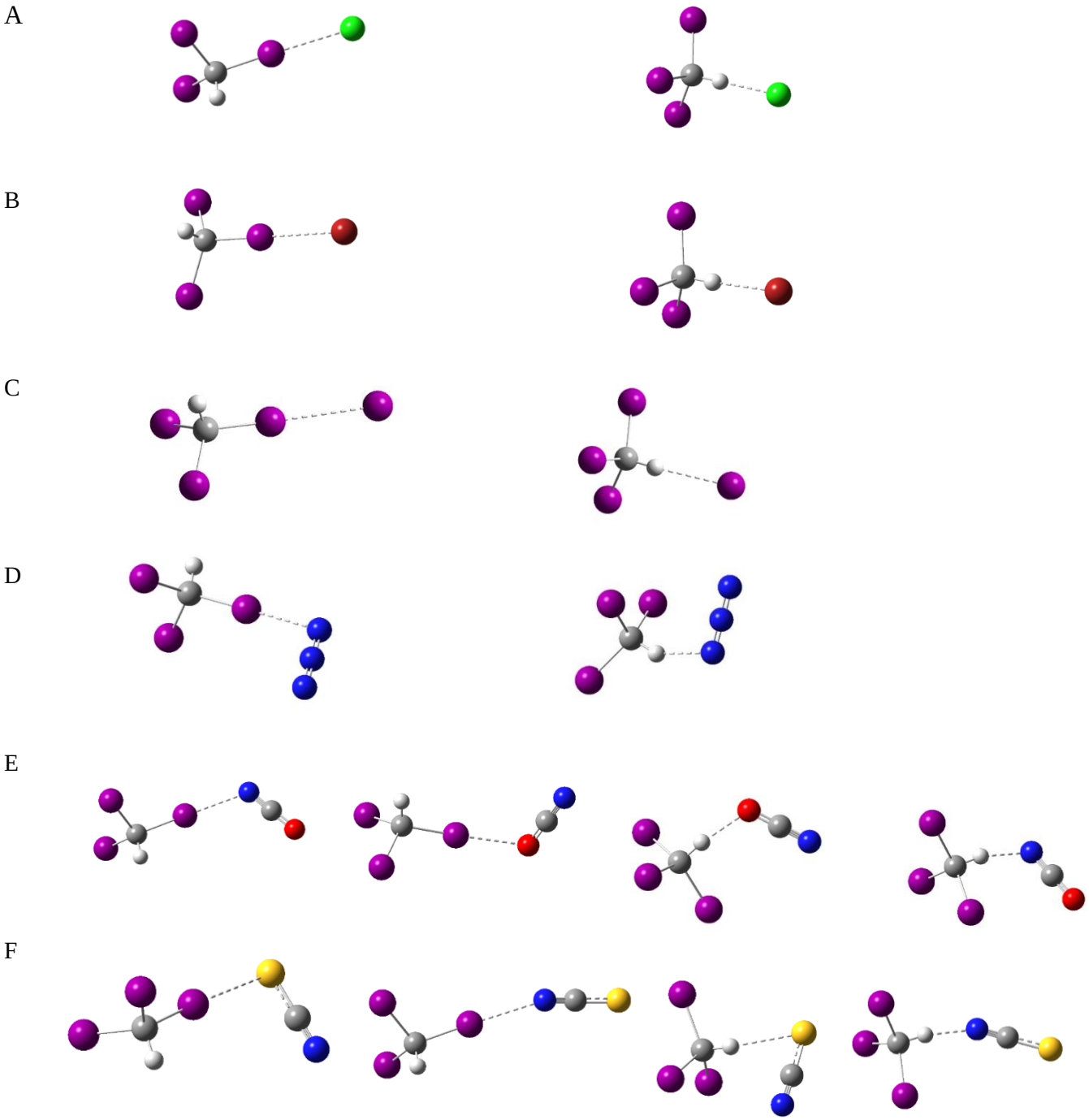

Figure S20. Structures of the [CHI_3, A^-] complexes resulting from the M06-2X/def-TZVPP computations (CH_3CN): A^- = Cl^- (A), Br^- (B), I^-(C) , N_3^- (D), NCO^-(E), NCS^-(F).

Table S3A. Energies of the XB and HB [CHI_3, A^-] complexes resulting from the M06-2X/def-TZVPP computations (CH_3CN).[a]

CHX_3	A	E, Hartree		ΔE, kcal/mol[b]		BSSE, Hartree	
		XB	HB	XB	HB	XB	HB
CHI_3	Cl	-1391.96176	-1391.96060	-3.98	-3.01	0.00292	0.00317
	Br	-3505.96671	-3505.96569	-3.80	-2.93	0.00168	0.00201
	I	-1229.40704	-1229.40601	-3.75	-2.88	0.00050	0.00079
	N_3	-1095.92156	-1095.91918	-5.17	-3.49	0.00106	0.00127
	NCS-S[c]	-1422.78923	-1422.78873	-3.85	-3.33	0.00077	0.00091
	NCS-N[c]	-1422.78815	-1422.78686	-3.12	-2.95	0.00078	0.00064
	NCO-O[c]	-1099.82489	-1099.82489	-3.59	-2.74	0.00080	0.00109
	NCO-N[c]	-1099.82666	-1099.82545	-4.67	-3.87	0.00092	0.00108
$CHBr_3$	Cl	-8221.64791	-8221.65107	-1.65	-3.28	0.00209	0.00288
	Br	-10335.65365	-10335.65605	-1.74	-2.90	0.00117	0.00188
	I	-8059.09456	-8059.09627	-1.82	-2.70	0.00036	0.00074
	N_3	-7925.60755	-7925.60937	-2.33	-3.56	0.00079	0.00112
	NCS-S[c]	-8252.47668	-8252.47890	-1.98	-3.12	0.00059	0.00084
	NCS-N[c]	-8252.47560	-8252.47814	-1.33	-2.79	0.00050	0.00068
	NCO-O[c]	-7929.51237	-7929.51453	-1.75	-2.83	0.00073	0.00107
	NCO-N[c]	-7929.51283	-7929.51500	-2.06	-2.77	0.00069	0.00102
$CHCl_3$	Cl	-1879.66466	-1879.66960	-0.52	-2.93	0.00140	0.00260
	Br	-3993.67076	-3993.67463	-0.66	-2.62	0.00081	0.00161
	I	-1717.11205	-1717.11497	-0.77	-2.41	0.00026	0.00057
	N_3	-1583.62450	-1583.62837	-1.11	-3.24	0.00058	0.00111
	NCS-S[c]	-1910.49423	-1910.49701	-1.04	-2.55	0.00042	0.00075
	NCS-N[c]	-1910.49398	-1910.49699	-0.91	-2.68	0.00036	0.00062
	NCO-O[c]	-1587.52994	-1587.53334	-0.83	-2.75	0.00053	0.00097
	NCO-N[c]	-1587.53000	-1587.53479	-0.90	-3.76	0.00051	0.00089

a) Energies of the separate trihalomethanes CHI3 -931.58196 CHBr3 -7761.27261 CHCl3 -1419.29184 Hartree.

b) $\Delta E = E_{comp} - (E_{CHX3} + E_A) + BSSE$ where E_{comp}, E_{CHX3} and E_A are sums of the electronic and ZPE of the complex, CHX_3 and anion and BSSE is a basis set superposition error.

c) HB- or XB- bonded atom of anion (see structures in Figure S19).

Table S3B. Energies of the XB and HB [CHI_3, A^-] complexes resulting from the M06-2X/def-TZVPP computations (gas phase).[a]

CHX_3	A	Energy		ΔE, kcal/mol[b]		BSSE	
		XB	HB	XB	HB	XB	HB
CHI_3	Cl	-1391.87941	-1391.86990	-25.95	-20.37	0.00350	0.00361
	Br	-3505.88621	-3505.87850	-21.75	-17.02	0.00202	0.00222
	I	-1229.33010	-1229.32380	-18.08	-14.17	0.00060	0.00075
	N_3	-1095.84680	-1095.83690	-22.72	-17.12	0.00150	0.00132
	NCS-S[c]	-1422.71446	-1422.70807	-16.53	-12.51	0.00089	0.00097
	NCS-N[c]	-1422.71284	-1422.70925	-15.37	-13.36	0.00084	0.00073
	NCO-O[c]	-1099.74208	-1099.73738	-16.97	-14.32	0.00122	0.00109
	NCO-N[c]	-1099.75083	-1099.74374	-22.27	-18.37	0.00143	0.00121
$CHBr_3$	Cl	-8221.55283	-8221.55998	-15.51	-20.09	0.00253	0.00322
	Br	-10335.56207	-10335.56862	-12.57	-16.35	0.00145	0.00204
	I	-8059.00814	-8059.01376	-10.01	-13.50	0.00042	0.00068
	N_3	-7925.52136	-7925.52743	-12.78	-16.81	0.00094	0.00126
	NCS-S[c]	-8252.39390	-8252.39845	-9.38	-12.15	0.00070	0.00091
	NCS-N[c]	-8252.39303	-8252.40079	-8.71	-13.72	0.00060	0.00074
	NCO-O[c]	-7929.42203	-7929.42870	-10.29	-14.64	0.00077	0.00107
	NCO-N[c]	-7929.42585	-7929.43464	-12.64	-18.50	0.00085	0.00104
$CHCl_3$	Cl	-1879.56099	-1879.57702	-8.81	-18.45	0.00165	0.00290
	Br	-3993.57222	-3993.58611	-6.92	-15.16	0.00089	0.00184
	I	-1717.02004	-1717.03186	-5.23	-12.47	0.00022	0.00066
	N_3	-1583.53130	-1583.54540	-6.76	-15.81	0.00073	0.00113
	NCS-S[c]	-1910.40558	-1910.41677	-4.51	-11.38	0.00049	0.00091
	NCS-N[c]	-1910.40664	-1910.41943	-5.11	-13.14	0.00039	0.00067
	NCO-O[c]	-1587.43523	-1587.44743	-6.32	-14.03	0.00069	0.00102
	NCO-N[c]	-1587.43676	-1587.45262	-7.34	-17.50	0.00063	0.00093

a) Energies of the separate trihalomethanes arte: CHI3 -931.57855CHBr3 -7761.26960CHCl3 -1419.28913 Hartree. b) $\Delta E = E_{comp} - (E_{CHX3} + E_A) + BSSE$ where E_{comp}, E_{CHX3} and E_A are sums of the electronic and ZPE of the complex, CHX_3 and anion and BSSE is a basis set superposition error. c) HB- or XB-bonded atom of the anion (see structures in Figure S19).

Table S4. Bond distances and angles in XB and HB complexes.[ab]

CHX_3	A	CH_3CN				Gas phase			
		Distance		Angle		Distance		Angle	
		XB	HB	XB	HB	XB	HB	XB	HB
CHI_3	Cl	3.111	2.259	178.2	179.9	2.726	1.980	176.9	179.6
	Br	3.312	2.460	178.6	173.7	2.928	2.205	176.9	179.4
	I	3.569	2.726	178.3	161.4	3.166	2.467	176.6	178.8
	N_3	2.767	2.110	179.5	149.6	2.448	1.726	176.6	175.4
	NCS-S[c]	3.281	2.652	176.6	153.0	2.911	2.323	177.7	174.9
	NCS-N[c]	2.918	2.072	178.2	169.5	2.573	1.841	176.9	178.5
	NCO-O[c]	2.835	2.015	175.0	158.6	2.516	1.730	178.4	173.2
	NCO-N[c]	2.810	2.014	176.0	164.5	2.443	1.702	177.8	178.5
$CHBr_3$	Cl	3.184	2.250	178.3	178.3	2.787	2.009	176.3	179.5
	Br	3.379	2.449	177.4	176.6	3.016	2.247	175.9	179.4
	I	3.615	2.709	176.9	163.9	3.302	2.507	175.5	179.3
	N_3	2.924	1.987	176.0	178.8	2.526	1.752	176.6	173.9
	NCS-S[c]	3.360	2.646	175.3	150.5	3.055	2.355	174.2	178.3
	NCS-N[c]	2.977	2.084	179.1	159.6	2.715	1.857	176.8	179.8
	NCO-O[c]	2.880	2.006	177.3	156.3	2.594	1.741	176.9	171.7
	NCO-N[c]	2.973	1.729	178.1	179.7	2.584	1.728	177.6	179.7
$CHCl_3$	Cl	3.271	2.279	178.5	179.0	2.923	2.056	175.8	179.4
	Br	3.457	2.508	177.6	163.0	3.158	2.281	175.8	179.6
	I	3.681	2.788	177.7	152.5	3.431	2.590	176.0	179.4
	N_3	2.990	2.121	175.1	148.3	2.691	1.805	174.3	174.3
	NCS-S[c]	3.415	2.782	174.3	143.7	3.179	2.401	174.5	175.6
	NCS-N[c]	3.127	2.088	177.8	165.1	2.780	1.898	174.9	180.0
	NCO-O[c]	2.933	2.012	176.1	158.0	2.669	1.778	171.7	172.1
	NCO-N[c]	3.113	1.977	176.9	177.0	2.691	1.777	176.1	179.9

a) M06-2X/def-TZVPP computations. b) Distances (X...A or H...A), in Å, angles (C-X-A or C-H-A) in deg, c c) HB- or XB-bonded atom of the anion (see structures in Figure S19).

Table S5. Calculated UV and NMR spectral characteristics of XB and HB complexes[a)]

CHX_3	A	λ, nm		log ε[b]			Δδ, ppm	
		XB	HB	XB	EXP[c]	HB	XB	HB
CHI_3	Cl	303	302	3.76	3.60	3.27	-0.608	2.907
	Br	306	303	3.86	3.98	3.34	-0.543	2.254
	I	314	318	4.06	4.06	3.40	-0.488	1.415
	N_3	328	386	4.02	3.90	2.93	-0.639	2.334
	NCS-S	311	329	4.02	3.95	2.81	-0.455	0.979
	NCO-N	360	302	3.90	3.91	3.22	-0.534	2.817
$CHBr_3$	Cl	229	240	3.83	3.99	3.16	-0.353	3.143
	Br	235	244	4.00		3.23	-0.306	2.581
	I	249	259	4.11		3.39	-0.276	1.872
	N_3	280	288	3.80		3.04	-0.261	2.831
	NCS-S	251	263	3.96		2.63	-0.217	0.992
	NCO-N	231	236	3.85		2.95	-0.277	3.128
$CHCl_3$	Cl	186	194	3.86		3.08	-0.343	2.993
	Br	192	270	3.92		3.08	-0.316	2.240
	I	204	209	3.98		3.34	-0.306	1.506
	N_3	234	239	3.52		2.75	-0.249	2.279
	NCS-S	209	211	3.81		2.60	-0.239	0.866
	NCO-N	195	188	3.72		2.84	-0.251	2.666
Δ				0.77[d]	0.01[e]	-0.05[f]		

a) From TD DFT and GIAO computations using CH_3CN-optimized structures. b) Note the calculated values of log ε for the separate CHI_3, $CHBr_3$ and $CHCl_3$ molecules are 3.45, 3.08 and 2.81, respectively. c) Experimental values (Table S1) d) $\Delta = 1/n(\Sigma (\log \varepsilon_{XB} - \log \varepsilon_o)$ where ε_{XB} and ε_o are extinction coefficients of the XB complex and the separate molecule, respectively. e) $\Delta = 1/n(\Sigma (\log \varepsilon_{XB} - \log \varepsilon(exp))$. f) $\Delta = 1/n(\Sigma (\log \varepsilon_{HB} - \log \varepsilon_o))$, where ε_{HB} and ε_o are extinction coefficients of the HB complex and the separate molecule, respectively.

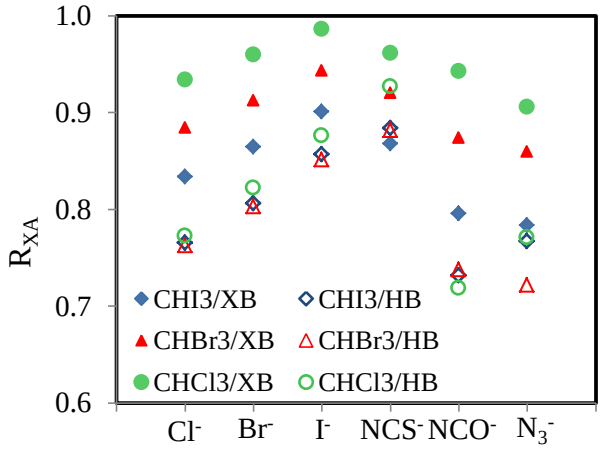

Figure S21. Normalized X…A and H...A separations in the calculated XB or HB complexes (as indicated). (R_{XA}= d_{XA}/(R_X + R_A), where d_{XA} are H…A or X…A separation, and R_X and R_A are van der Waals radii)

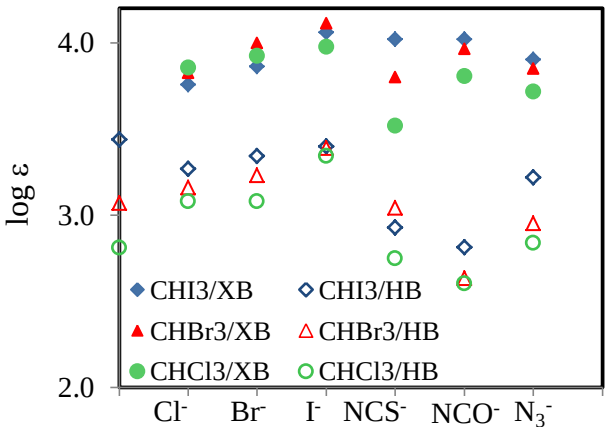

Figure S22. Calculated extinction coefficient of the XB and HB complexes $CHX_3 \cdot A^-$ (as indicated). The symbols on the y-axis show values for the separate CHX_3 molecules, for comparison.

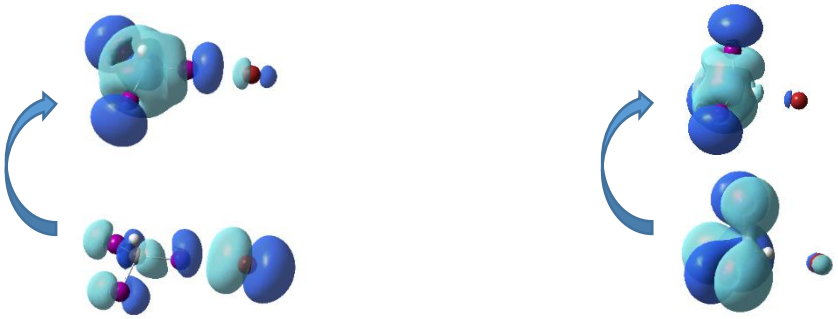

Figure S23. Main components of the most intense ground – excited state transition resulted from the TD DFT computations of the XB (left) and HB (right) complexes between CHI_3 and Br^-

Atomic coordinates of the XB and HB complexes [CHX_3, A^-] (M06-2X/def-TZVPP, CH_3CN).

CHI_3-Cl (XB)

I	1.50226100	-1.77178500	-0.08682800
I	1.50329000	1.77122400	-0.08690500
I	-1.58404400	0.00052400	0.17993700
C	0.52018500	0.00003700	0.59788300
H	0.64478300	0.00003700	1.67142200
Cl	-4.65328300	0.00010200	-0.32867500

CHI_3-Cl (HB)

I	-0.57185500	1.96603700	-0.39233200
C	0.00035200	-0.00044400	0.19429500
H	0.00374200	-0.00081100	1.28386400
I	1.98671000	-0.48912900	-0.40000500
I	-1.41949200	-1.47662000	-0.39042000
Cl	0.01411200	-0.00069300	3.54332300

CHI_3-Br (XB)

I	-1.94827200	1.77169900	-0.10883000
I	-1.94836900	-1.77163600	-0.10884500
I	1.12309900	-0.00006800	0.25483200
C	-0.99209800	-0.00000200	0.60766900
H	-1.14496400	0.00000100	1.67746400
Br	4.40272300	0.00000900	-0.20836600

CHI_3-Br (HB)

I	0.97407000	0.20214200	1.96622700
C	0.16003300	0.00058900	0.00892800
H	-0.92044400	0.01348200	0.12711700
I	0.62918800	-1.87321100	-0.88927900
I	0.62630400	1.65464600	-1.24946400
Br	-3.37733100	0.02438500	0.25607600

CHI_3-I (XB)

I	-2.36733600	1.77178000	-0.12005300
I	-2.36679100	-1.77209500	-0.11998100
I	0.69610200	0.00031500	0.28571300
C	-1.42390700	-0.00000500	0.60912900
H	-1.58583700	-0.00000600	1.67753500
I	4.22914400	0.00000000	-0.14628900

CHI_3-I (HB)

I	1.79443300	-0.00620600	1.74589600
C	0.51120700	-0.00014500	0.04492500
H	-0.50867600	0.00031500	0.41667700
I	0.69313500	-1.76952400	-1.12716700
I	-3.23352800	0.00031600	0.48572900
I	0.69768500	1.77542500	-1.11740600

CHI_3-N_3 (XB)

C	-0.69981300	-0.00117800	-0.64278600
N	4.45963200	0.00120700	0.71802900
N	4.21545300	-0.03931200	-0.43188700
N	4.69472700	0.04133500	1.85194400
H	-0.99453700	-0.00314800	-1.68279100
I	1.45116600	-0.02041400	-0.56147700
I	-1.54355300	1.78119800	0.18390300
I	-1.57544900	-1.76101800	0.19970400

CHI_3-N_3 (HB)

C	-0.16149000	-0.00014000	0.29335200
N	2.93676300	-0.00012600	1.78845900
N	2.00815200	-0.00097600	2.50293000
N	3.86085600	0.00060100	1.08085500
H	0.28636500	0.00002600	1.28350600
I	0.56559200	-1.76988600	-0.64309300
I	0.56507300	1.77027300	-0.64271000
I	-2.28081300	-0.00030600	0.51883400

CHI_3-NCS S-(XB)

C	0.79134700	-0.00965600	0.56418200
N	-5.11769200	-0.21122100	1.74553400
H	0.77127300	-0.02680800	1.64448700
S	-4.40898200	0.12782100	-0.96703700
C	-4.82770900	-0.07136200	0.62736700
I	-1.24171600	0.05067800	-0.11391700
I	1.80375100	-1.79667000	-0.02312900
I	1.88729400	1.74497900	0.03251900

CHI_3-NCS S-(HB)

C	-0.11145700	-0.00868800	-0.10747000
N	2.93578200	1.53013900	-1.28069800
S	2.83646600	-1.22651200	-1.87997700
C	2.91266700	0.39326100	-1.53423700
H	0.64761400	-0.12117000	-0.87010000
I	0.92563400	-0.09004900	1.75095800
I	-1.05569800	1.87083400	-0.44154900
I	-1.44331000	-1.65386100	-0.37044900

CHI_3-NCS N-(XB)

C	1.04731900	0.00582500	0.59896400
N	-3.92174100	-0.40879800	-0.20691200
H	1.19286700	0.00935100	1.66962800
C	-5.06277400	-0.17037300	-0.19415900
S	-6.68070700	0.16370800	-0.17905400
I	-1.04477800	-0.18957000	0.22634300
I	1.83428800	1.86869000	-0.09418500
I	2.17734500	-1.65609800	-0.12810500

CHI_3-NCS N-(HB)

C	0.28230200	-0.00009800	-0.10347000
N	-2.64307800	0.00393100	-1.25065400
C	-3.79430400	0.00204700	-1.06581200
S	-5.42668400	-0.00268900	-0.80754600
H	-0.67309900	-0.00141700	-0.61859600
I	-0.19376700	-0.01061600	1.97276900
I	1.29058500	1.77893900	-0.70176700
I	1.30079600	-1.76822400	-0.71799000

CHI_3-NCO O-(XB)

C	-0.58360900	0.00001000	0.56458100
H	-0.56778100	-0.00000500	1.64488900
C	4.88089700	0.00004300	0.07895500
O	4.16154400	-0.00020500	-0.90932200
N	5.56977100	0.00022800	1.03322800
I	1.44077200	0.00023100	-0.11252300
I	-1.63994600	-1.77127100	0.00472200
I	-1.64038600	1.77103600	0.00470400

CHI_3-NCO O-(HB)

C	-0.08455300	-0.00376100	0.20621800
C	3.15588600	0.16368800	2.08318200
O	2.04324900	0.61532300	2.30256500
N	4.23078800	-0.27138400	1.87570000
H	0.52631800	0.05460000	1.10049900
I	1.28695800	-0.38274000	-1.37994700
I	-1.03205800	1.89653600	0.02525200
I	-1.47972700	-1.58996700	0.47946200

CHI_3-NCO N-(XB)

C	-0.60434800	-0.00469600	0.56770400
N	4.12118800	0.14529500	-0.91186000
H	-0.60603600	-0.01186700	1.64842800
C	4.92049500	0.01599800	-0.04824700
O	5.73855800	-0.11525000	0.83215700
I	1.43402000	0.05709700	-0.09590000
I	-1.61283000	-1.80051400	-0.01038900
I	-1.70888200	1.74056800	0.01120500

CHI_3-NCO N-(HB)

C	-0.10761900	0.00120800	-0.22079400
N	1.95669900	-0.20531100	-2.49383900
C	3.05449000	-0.06248400	-2.07773400
O	4.18258400	0.08293600	-1.65933000
H	0.47849000	-0.02025700	-1.13911400
I	-1.65961200	1.43647200	-0.48271000
I	1.28053600	0.56208500	1.29535500
I	-0.85332600	-1.97664000	0.04889800

$CHBr_3$-Cl (XB)

C	0.71580800	-0.00007700	0.56512000
H	0.86674800	-0.00022800	1.63431200
Br	-1.18299600	0.00004100	0.22106000
Br	1.56983300	1.59414500	-0.12071000
Br	1.56969900	-1.59418600	-0.12114300
Cl	-4.33178600	0.00004100	-0.25278000

$CHBr_3$-Cl (HB)

C	0.01906700	-0.00058500	-0.01172400
Br	-0.52270700	1.82838300	0.28095600
Br	-0.43019500	-1.12096000	1.49413300
Cl	3.35131800	-0.01428800	-0.23481700
Br	-0.70970800	-0.70020100	-1.65597900
H	1.10456100	-0.00638100	-0.10665500

$CHBr_3$-Br (XB)

C	1.30510400	-0.00000100	0.56626300
H	1.46999800	0.00000800	1.63336600
Br	-0.60027600	-0.00002100	0.25594300
Br	2.14544600	1.59415600	-0.13298700
Br	2.14548300	-1.59413500	-0.13299200
Br	-3.95638600	0.00000000	-0.13370600

$CHBr_3$-Br (HB)

C	0.44006700	-0.00039800	-0.00977100
Br	0.96024600	1.71075500	0.71390900
Br	1.13320700	-0.25739000	-1.79171300
Br	-3.09360700	-0.00481700	-0.08026900
H	-0.64511100	-0.00412400	-0.07618900
Br	0.94314700	-1.44836200	1.16192500

$CHBr_3$-I (XB)

C	-1.81940000	0.00000100	0.56551400
H	-1.98891400	0.00000900	1.63185000
Br	0.08958800	0.00000300	0.27000800
Br	-2.65216500	-1.59421500	-0.13959300
Br	-2.65217900	1.59420900	-0.13959400
I	3.68720300	0.00000100	-0.08874900

$CHBr_3$-I (HB)

C	-0.86129200	0.00012400	0.04425500
Br	-1.18425100	-1.60353700	-0.97800000
Br	-1.19055700	1.58540000	-1.00393600
I	2.90004300	0.00307700	0.18484000
Br	-1.87456600	0.01333700	1.68587700
H	0.19356100	0.00416600	0.30003300

$CHBr_3$-N_3 (XB)

Br	1.00979200	0.20184000	-0.65736200
Br	-1.45341700	-1.68090600	0.12427300
Br	-1.73829800	1.48603800	0.35572200
C	-0.91182000	0.02578800	-0.60549800
N	3.96173400	-0.02259600	0.54776000
N	3.92715700	0.37434800	-0.55337000
N	3.98561600	-0.41819600	1.64265300
H	-1.28334800	0.06639400	-1.61845600

$CHBr_3$-N_3 (HB)

Br	-0.36774800	-1.46989400	1.18701700
Br	-0.43858800	1.69564900	0.82676300
C	-0.14399000	-0.00234900	-0.05496300
N	3.55767500	-0.03876500	-0.68733700
N	2.48918800	-0.09086500	-1.18248500
N	4.61485700	0.01072300	-0.21945300
H	0.90753500	-0.02400200	-0.43255500
Br	-1.32725400	-0.20088600	-1.57414400

$CHBr_3$-NCS S-(XB)

Br	0.76626000	-0.00088500	-0.12713100
Br	-2.00093900	1.59455600	-0.00890600
Br	-2.00248300	-1.59367000	-0.00801800
C	-1.05039800	0.00015400	0.52713200
N	4.42077400	0.00190000	1.78876000
H	-1.01491200	0.00037800	1.60620900
S	4.00945700	-0.00115500	-1.00413000
C	4.25353600	0.00064100	0.63627700

$CHBr_3$-NCS S-(HB)

Br	-1.25438100	-1.51134900	0.78456300
Br	-1.25520100	1.66126300	0.44275200
C	-0.31214500	0.01691000	0.08086300
N	2.81508300	-1.74905800	0.49881800
S	3.10087100	1.04836000	0.74310600
C	2.95279600	-0.59658700	0.59984900
Br	0.05798700	-0.18236800	-1.80018600
H	0.64239900	0.08360900	0.58476000

$CHBr_3$-NCS N-(XB)

Br	-0.50576800	-0.00029200	0.11502200
Br	2.25333000	-1.59390700	-0.08129400
Br	2.25276700	1.59425400	-0.08131900
C	1.36708100	0.00003900	0.56072500
N	-3.41199300	-0.00063000	-0.52882700
H	1.46008700	0.00004300	1.63637800
C	-4.54592400	-0.00031500	-0.25877700
S	-6.15716200	0.00025600	0.11996300

$CHBr_3$-NCS N-(HB)

Br	-1.91149000	0.26771000	1.50718700
Br	-0.64544700	1.44679000	-1.17259500
C	-0.61291900	0.00122700	0.10502500
N	2.44773500	-0.05081500	0.74617900
C	3.59952800	-0.02288700	0.56918100
S	5.23305100	0.01558800	0.32067800
Br	-0.84764000	-1.70761300	-0.76164500
H	0.37761100	-0.00482100	0.54752100

$CHBr_3$-NCO O-(XB)

Br	1.00097800	0.36177900	0.01692600
Br	-2.03039600	1.36284800	0.01112200
Br	-1.38480500	-1.75651800	-0.12189900
C	-0.80792200	-0.03653700	0.54498500
H	-0.84083200	-0.08888500	1.62283300
C	4.33002300	0.01711700	-0.04058500
O	3.74930400	0.89147100	-0.66102500
N	4.88737000	-0.83002300	0.56053900

$CHBr_3$-NCO O-(HB)

Br	-1.50986000	1.30808400	-0.77573800
Br	-1.04729600	-1.74245800	0.03145100
C	-0.23542500	-0.00145700	-0.15679800
C	3.33618600	-0.17157300	-1.11271000
O	2.33791500	-0.66664700	-1.61181200
N	4.30067800	0.30533100	-0.63353900
Br	0.61524100	0.55808700	1.48257100
H	0.55437300	-0.09592800	-0.89364300

$CHBr_3$-NCO N-(XB)

Br	1.02760500	-0.07020900	-0.15601500
Br	-1.67735100	1.62922100	-0.02322400
Br	-1.79856400	-1.55587400	0.03019300
C	-0.77483700	0.00870300	0.52447500
N	3.83990400	-0.17046900	-1.11377200
H	-0.72874600	0.02479500	1.60303600
C	4.31248200	-0.01784900	-0.04116300
O	4.78929800	0.13919000	1.06376400

$CHBr_3$-NCO N-(HB)

C	-0.17842400	-0.00140100	-0.01014900
N	2.66441300	-0.01245200	-0.14806800
C	3.84469500	-0.01116900	-0.10229600
O	5.05312400	-0.00977700	-0.05809800
H	0.93767200	-0.00775200	-0.06754800
Br	-0.68802800	-0.30143900	1.83243800
Br	-0.80420900	1.72486700	-0.62170300
Br	-0.85094000	-1.41632600	-1.14663600

$CHCl_3$--Cl (XB)

C	1.18816600	-0.00000300	0.49801900
H	1.38388400	0.00000600	1.56113900
Cl	-3.80202300	-0.00000200	-0.13753300
Cl	-0.55394600	0.00028700	0.24505200
Cl	1.92784800	1.45135200	-0.18760400
Cl	1.92736400	-1.45163700	-0.18751900

$CHCl_3$-Cl (HB)

C	0.40176800	-0.00035100	-0.00294000
Cl	-2.96621800	-0.00322700	-0.01792600
Cl	0.93666700	-1.10783700	1.26450100
Cl	0.94414500	1.64530400	0.33793600
H	-0.68767600	-0.00354300	-0.02029800
Cl	0.98405800	-0.53390800	-1.58228000

$CHCl_3$-Br (XB)

C	2.00120400	-0.00000500	0.49716800
H	2.20274900	-0.00002200	1.55919000
Br	-3.18577300	0.00000500	-0.06706500
Cl	2.73342300	1.45151900	-0.19369500
Cl	0.25587200	-0.00022700	0.25834800
Cl	2.73376900	-1.45130000	-0.19376700

$CHCl_3$-Br (HB)

C	1.05830000	-0.00043700	-0.04504100
Br	-2.50273100	-0.00048600	-0.11247600
Cl	1.99565100	-0.07345600	-1.53861900
Cl	1.37788200	-1.41287600	0.96379000
Cl	1.40567100	1.48756500	0.83932600
H	-0.00070100	-0.00131200	-0.28953800

$CHCl_3$-I (XB)

C	2.63006900	0.00000600	0.49640200
H	2.83909900	-0.00000200	1.55696500
I	-2.78600600	-0.00000100	-0.04438400
Cl	3.35434100	-1.45150700	-0.20071500
Cl	3.35491200	1.45116800	-0.20082700
Cl	0.88126500	0.00033900	0.27313000

$CHCl_3$-I (HB)

C	1.58084800	-0.00000100	0.07530300
I	-2.20297900	0.00000000	0.10240400
Cl	1.78840500	-1.45127100	-0.90570900
Cl	1.78836700	1.45120800	-0.90581100
Cl	2.70027600	0.00006300	1.43913200
H	0.56299700	-0.00000100	0.45136600

$CHCl_3$-N_3 (XB)

C	-1.39365200	-0.08293000	-0.51425100
N	3.33388000	0.04224400	0.26543600
N	3.32387900	-0.55562400	-0.73943700
N	3.33608300	0.63900200	1.26749400
H	-1.85109900	-0.23608600	-1.48159100
Cl	0.34384600	-0.31866500	-0.66881000
Cl	-1.76391700	1.56551400	0.00378500
Cl	-2.09427500	-1.25541800	0.60694600

$CHCl_3$-N_3 (HB)

C	0.66148500	-0.00060600	-0.15998500
N	-2.65926000	-0.00293700	-0.54207500
N	-2.09724400	-0.01222200	-1.57035300
N	-3.21731600	0.00626100	0.47911800
H	-0.06342300	-0.00444400	-0.96957300
Cl	0.37618200	-1.44685300	0.81128100
Cl	0.37862000	1.45643100	0.79595700
Cl	2.29880100	-0.00544000	-0.82120000

$CHCl_3$-NCS S-(XB)

C	-1.65575700	0.14786700	0.43863500
N	3.40165700	1.11108800	1.41255100
H	-1.63704700	0.49130300	1.46336100
S	3.30323600	-0.63756900	-0.80091700
C	3.36334500	0.38970800	0.49859900
Cl	-0.00212900	-0.19213200	-0.06630000
Cl	-2.36541200	1.42720700	-0.55042800
Cl	-2.64845100	-1.31114900	0.37202500

$CHCl_3$-NCS S-(HB)

C	-0.84222500	0.00687800	-0.00186700
N	2.22254500	1.97631600	-0.01108300
S	2.78103000	-0.78952100	-0.00368300
C	2.47717100	0.83884500	-0.00795100
H	0.20723200	0.26767400	-0.01254200
Cl	-1.78669200	1.49676400	-0.02950900
Cl	-1.17527100	-0.97264500	-1.43027100
Cl	-1.15987200	-0.90905400	1.47201300

$CHCl_3$-NCS N-(XB)

C	1.66580900	0.14692100	0.46099700
N	-2.73167700	-1.54278600	-0.83359300
H	1.61604100	0.40289200	1.50997100
C	-3.16215100	-0.59453000	-0.30975600
S	-3.76105200	0.75597700	0.43825700
Cl	0.08703700	-0.44386900	-0.04469200
Cl	2.89946600	-1.10176500	0.26557600
Cl	2.11117800	1.60367000	-0.43231900

$CHCl_3$-NCS N-(HB)

C	-1.33495900	0.00013400	-0.04451400
N	1.80950200	0.02527500	-0.43251600
C	2.95236500	0.01163300	-0.24742000
S	4.58372000	-0.00536100	0.01424800
H	-0.28178600	0.00742600	-0.30632500
Cl	-1.98397300	-1.60736500	-0.37943500
Cl	-1.46240300	0.37620800	1.67631700
Cl	-2.16707600	1.22120500	-1.01114200

$CHCl_3$-NCO O-(XB)

C	-1.30391000	0.07269100	0.48173900
H	-1.35951100	0.18957000	1.55484300
C	3.58740600	-0.00811800	-0.03147500
O	3.14421500	-1.04059300	-0.50109000
N	4.01407400	0.99318000	0.42362700
Cl	0.34018400	-0.38085200	0.05119400
Cl	-2.45037800	-1.18811100	0.01455500
Cl	-1.74825800	1.61575600	-0.25475500

$CHCl_3$-NCO O-(HB)

C	0.68612700	-0.01618100	-0.09212400
C	-3.00655700	-0.20564600	-0.39507300
O	-2.11902100	-0.84436100	-0.93813600
N	-3.86425100	0.40899200	0.12828000
H	-0.21627100	-0.26260400	-0.64189100
Cl	0.22346700	1.07184300	1.21998900
Cl	1.83868100	0.76731900	-1.17514700
Cl	1.35789800	-1.51648400	0.55352300

$CHCl_3$-NCO N-(XB)

C	-1.25914000	0.04559500	0.46023000
N	3.31321800	-0.40102700	-1.15906400
H	-1.20166400	0.14671700	1.53485400
C	3.55971800	-0.03181100	-0.06470100
O	3.80597100	0.34868200	1.06316300
Cl	0.37126300	-0.14594900	-0.17392000
Cl	-2.01856100	1.50675600	-0.18094200
Cl	-2.24929600	-1.37326000	0.10192700

$CHCl_3$-NCO N-(HB)

C	0.78028000	-0.00951900	-0.03246600
N	-2.22781700	-0.27496000	-0.55423900
C	-3.35020400	-0.10055700	-0.22964300
O	-4.50272400	0.07622200	0.10091400
Cl	1.35103900	-1.55984400	0.59447000
Cl	1.66361600	0.42975100	-1.49824400
Cl	0.94497500	1.25263300	1.19330000
H	-0.27765200	-0.10778600	-0.27692700

X-ray Structural Analysis

Co-crystals of CHI_3 with Bu_4NI, Pr_4NBr or Pr_4NCl were crystallized by diffusion of hexane into dichloromethane solutions containing 1:1 mixtures of the CHI_3 and alkylammonium salt of halide at low temperatures (-30 °). Intensity data for X-ray crystallographic analysis were collected at 173 K with a Bruker SMART Apex or Bruker AXS D8 Quest CMOS diffractometer using Mo Kα radiation (λ= 0.71073 Å). The structures were solved by direct methods and refined by full matrix least-squares treatment. Intermolecular contacts were analyzed using the OLEX2 structure solution, refinement and analysis program. Crystallographic, data collection and structure refinement details, as well as geometric characteristics of the halogen bonds in these crystals are presented in Table S5. Complete crystallographic data, in CIF format, have been deposited with the Cambridge Crystallographic Data Centre. CCDC 1837582, 1837583 and 1837584 contain the supplementary crystallographic data for this paper. These data can be obtained free of charge via www.ccdc.cam.ac.uk/data_request/cif.

Table S6. Crystallographic, data collection and structure refinement details

	CHI_3·Br	CHI_3·Cl	CHI_3·I
Chemical formula	$C_{12}H_{28}N$·CHI_3·Br	$C_{12}H_{28}N$·CHI_3·Cl	$C_{16}H_{36}N$·CHI_3·I
M_r	659.98	615.52	763.07
Crystal system, space group	Monoclinic, *Pn*	Monoclinic, *Pn*	Orthorhombic, *Pbca*
Temperature (K)	100	100	100
a, *b*, *c* (Å)	8.7748 (6), 8.9163 (7), 13.3043 (10)	8.7174 (5), 8.8068 (5), 13.2169 (7)	15.9191 (6), 17.5775 (7), 17.8152 (6)
β (°)	98.065 (3)	97.763 (3)	
V (Å^3)	1030.62 (13)	1005.39 (10)	4985.0 (3)
Z	2	2	8
Radiation type	Mo *K*α	Mo *K*α	Mo *K*α
μ (mm^{-1})	6.48	4.79	5.00
Crystal size (mm)	0.31 × 0.26 × 0.04	0.52 × 0.25 × 0.07	0.53 × 0.33 × 0.13
T_{min}, T_{max}	0.429, 0.746	0.623, 0.729	0.409, 0.747
No. of measured, independent and observed [$I > 2\sigma(I)$] refls	9213, 5325, 5206	24409, 3359, 3228	67764, 7607, 6492
R_{int}	0.062	0.080	0.039
$(\sin\theta/\lambda)_{max}$ (Å^{-1})	0.704	0.602	0.714
$R[F^2 > 2\sigma(F^2)]$, $wR(F^2)$, *S*	0.052, 0.134, 1.06	0.029, 0.061, 1.08	0.035, 0.080, 1.30
No. of reflections	5325	3359	7607
No. of parameters	167	167	204
No. of restraints	2	2	
H-atom treatment	H-atom parameters constrained	H-atom parameters constrained	H-atom parameters constrained

[1]Diffractometer: Bruker Kappa *APEX* CCD area detector Absorption correction: Multi-scan *SADABS2012*/1 (Bruker,2012) was used for absorption correction. wR2(int) was 0.1254 before and 0.0869 after correction. The Ratio of minimum to maximum transmission is 0.5746. The l/2 correction factor is 0.0015. Computer programs: *APEX2* V2.1-4 (Bruker, 2007), *SAINT* V7.23A (Bruker, 2005), Bruker *SAINT*, *SHELXT* (Sheldrick, 2008), *SHELXL* (Sheldrick, 2008), Olex2 (Dolomanov *et al.*, 2009). [2] Diffractometer: Bruker Kappa *APEX* CCD area detector Absorption correction: Multi-scan *SADABS2012*/1 (Bruker,2012) was used for absorption correction. wR2(int) was 0.1182 before and 0.0970 after correction. The Ratio of minimum to maximum transmission is 0.8552. The l/2 correction factor is 0.0015.[3]Diffractometer: Bruker AXS D8 Quest CMOS diffractometer. Absorption correction: Multi-scan *SADABS* 2016/2: Krause, L., Herbst-Irmer, R., Sheldrick G.M. & Stalke D., J. Appl. Cryst. 48 (2015) 3-10.Computer programs: Apex3 v2016.9-0 (Bruker, 2016), *SAINT* V8.37A (Bruker, 2016), *SHELXS97* (Sheldrick, 2008), *SHELXL2016*/6 (Sheldrick, 2015, 2016), SHELXLE Rev714 (Hübschle *et al.*, 2011).

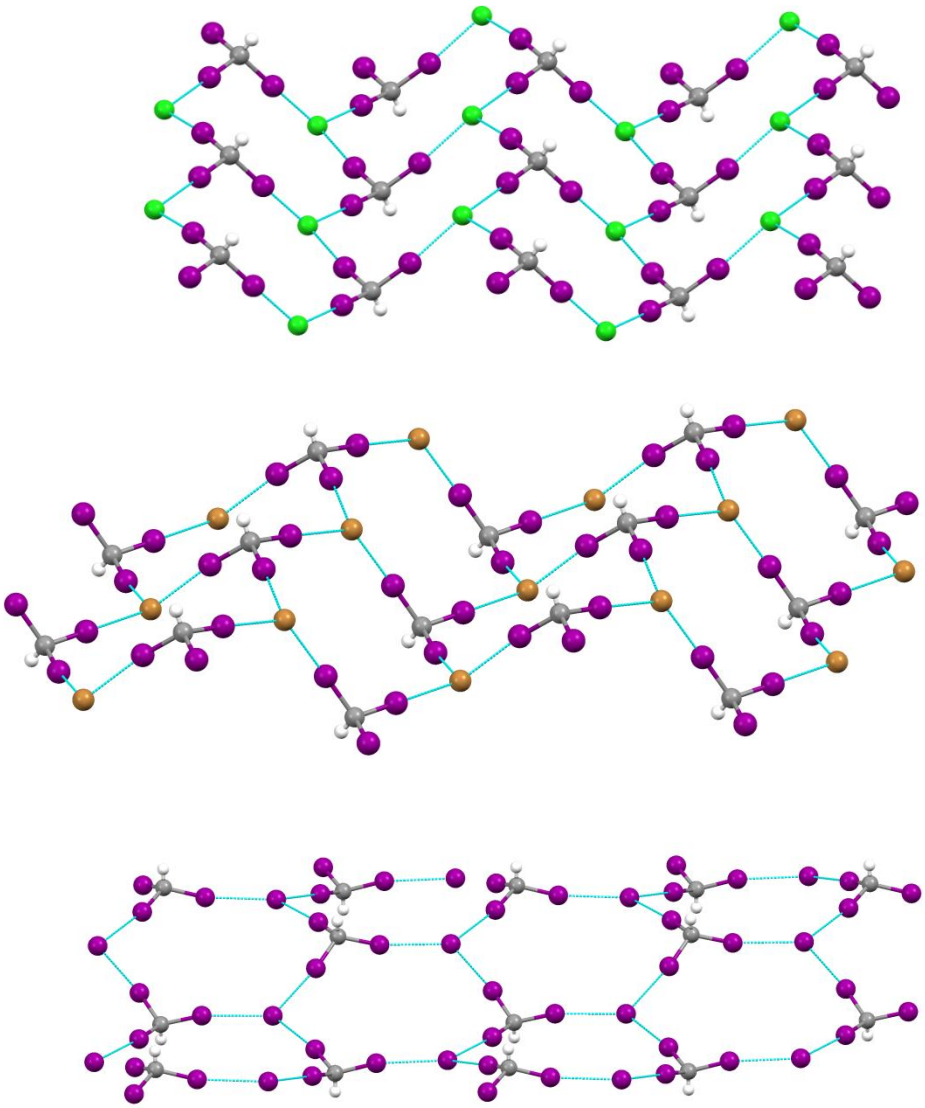

Figure S24. Halogen-bonded networks in the co-crystals of CHI_3 with Pr_4NCl (top), Pr_4NBr (middle) and Bu_4NI (bottom).

Table S7. Bond distances (I…X, in Å) and angles (C-I-A, in deg) in the halogen-bonded complexes in the solid-state structures in comparison with the calculated structures.

	X-ray crystallographic measurements		M06-2X/def-TZVPP computations (CH_3CN)	
A^-	$d_{I...X}$, Å[a]	∠C-I-A, deg [a]	$d_{I...X}$, Å[b]	∠C-I-A, deg[b]
I^-	3.518, 3.541, 3.594	170.21. 173.14, 166.29	3.551	178.3
Br^-	3.231, 3.243, 3.289	170.6, 168.46, 177.92	3.254	178.6
Cl^-	3.115, 3.124, 3.179	171.65, 169.99, 179.17	3.130	178.2